PRODUCTION OF LUNAR OXYGEN THROUGH VACUUM PYROLYSIS

JOHN MATCHETT

MAJOR RESEARCH REPORT - MAE 298

THE GEORGE WASHINGTON UNIVERSITY SCHOOL OF ENGINEERING & APPLIED SCIENCE - DEPARTMENT OF MECHANICAL AND AEROSPACE ENGINEERING

Report Documentation Page

Form Approved
OMB No. 0704-0188

1. REPORT DATE	2. REPORT TYPE	3. DATES COVERED
26 JAN 2006	**N/A**	**-**

4. TITLE AND SUBTITLE	5a. CONTRACT NUMBER
Production Of Lunar Oxygen Through Vacuum Pyrolysis	5b. GRANT NUMBER
	5c. PROGRAM ELEMENT NUMBER
6. AUTHOR(S)	5d. PROJECT NUMBER
	5e. TASK NUMBER
	5f. WORK UNIT NUMBER
7. PERFORMING ORGANIZATION NAME(S) AND ADDRESS(ES) **The George Washington University**	8. PERFORMING ORGANIZATION REPORT NUMBER
9. SPONSORING/MONITORING AGENCY NAME(S) AND ADDRESS(ES)	10. SPONSOR/MONITOR'S ACRONYM(S)
	11. SPONSOR/MONITOR'S REPORT NUMBER(S)

12. DISTRIBUTION/AVAILABILITY STATEMENT
Approved for public release, distribution unlimited

13. SUPPLEMENTARY NOTES
The original document contains color images.

14. ABSTRACT

15. SUBJECT TERMS

16. SECURITY CLASSIFICATION OF:			17. LIMITATION OF ABSTRACT	18. NUMBER OF PAGES	19a. NAME OF RESPONSIBLE PERSON
a. REPORT	b. ABSTRACT	c. THIS PAGE			
unclassified	**unclassified**	**unclassified**	**UU**	**70**	

Standard Form 298 (Rev. 8-98)
Prescribed by ANSI Std Z39-18

Table of Contents

I. Abstract

Increasing efficiency of future space exploration will require that missions utilize non-terrestrial resources for propellant manufacture. The vacuum pyrolysis method of oxygen production from lunar regolith presents a viable option for *in situ* propellant production because of its simple operation involving limited resources from earth.

Lunar regolith, the fine layer of pulverized rock across the entire lunar surface, is composed of approximately forty percent oxygen in the form of metal oxides. Employing concentrated solar radiation to heat raw regolith beyond its respective vaporization temperatures will dissociate the regolith minerals and agglutinates into reduced oxides and gaseous oxygen. Once dissociated, rapid quenching will cause the reduced oxides to condense, releasing gaseous oxygen to be isolated and stored.

Vacuum solar pyrolysis experiments involving terrestrial representatives of lunar regolith were completed at temperatures between 1000 ^{o}C and 2000 ^{o}C at a rough vacuum. A large Fresnel lens was employed to focus solar radiation on a small sample of regolith simulant, located in a vacuum chamber. Pyrolysis measurement data collected included pressure, temperature, mass loss, residual gas analysis, and scanning electron microscopy.

The savings gained from in situ oxidizer production are analyzed using the Apollo program as a case study. Approximately 50,000 lbs of launch propellant can be saved or an extra 9200 lbs of payload can be added by employing vacuum pyrolysis to provide oxidizer for the return journey from the Moon.

The complexity of the lunar environment presents new engineering challenges to a terrestrially proven pyrolysis system. The lunar pyrolysis oxygen production plant meets these challenges by a robust design that takes advantage of all the lunar resources. The technology readiness of an oxygen production plant will be demonstrated on an evolutionary path. Oxygen production yields are estimated at 6-23% of regolith mass depending upon oxide dissociation and condenser efficiency. This study provides an analysis of the infrastructure needed for an oxygen production plant through vapor phase pyrolysis on the lunar surface.

II. Introduction

As human space exploration continues, methods to improve efficiency and reduce mission costs are necessary to support larger and more complicated missions. Interplanetary exploration missions require vast amounts of fuel for propulsion. *In-situ* propellant production provides the enhanced ability of fueling or refueling for interplanetary missions. *In-situ* capacities refer to those that exist in the original position, in this case, resources that already exist on the lunar surface. This capability for *in situ* resource utilization (ISRU) translates into numerous mission design options including the addition of payload mass or reduction of the launch vehicle size. Just as aerial refueling was applied to increase the effectiveness of aircraft, so could propellant refueling through *in situ* utilization for long duration propulsion systems. The technology developed for lunar *in situ* missions, and the lessons learned, will transfer to future exploration missions and their respective destinations far beyond earth orbit.

Large-scale missions are hindered by the enormous energy requirements of space flight. It costs approximately $4,000 per pound to boost payload or propellant into low earth orbit[1]. *In-situ* propellant production (ISPP) reduces the burden of space transportation systems. Currently spacecraft must transport both outbound and return propellant for lunar missions. The investigation of *in-situ* propellant production from lunar resources, specifically lunar regolith, aims at harvesting oxygen. A common hydrogen-oxygen propulsion system operates at 6:1 oxidizer to fuel ratio while a hypergolic system of monomethyl-hydrazine and nitrogen tetroxide (MMH/NTO) operates at about 1.35:1 oxidizer ratio. In terms of propulsive requirements, *in-situ* oxygen provides mass savings between 50-86%. Not only will there be savings on the propellant necessary to return to Earth, but also on the propellant normally required to transport the return propellant to the Moon. In terms of operational costs, no matter how inexpensive it becomes to lift materials, supplies, and propellants from Earth, it will always be proportionally cheaper to set up a lunar production facility and obtain the required supplies from the Moon.[1] This comparison does not include costs of research, development and deployment of production infrastructure, but only compares operational scenarios. Launching materials from the lunar surface, $g = 1.6\ m/s^2$, requires about one twentieth the energy of launching materials from Earth, $g = 9.81\ m/s^2$. Since the change in velocity remains constant regardless of payload or launch vehicle, only reducing the final mass will drive the required initial mass in the form of propellant lower, as shown by the ideal rocket equation in Equation 1.

$$\Delta V = -V_{exit} \ln\left(\frac{m_{final}}{m_{initial}}\right) \tag{1}$$

In an effort to roadmap *in situ* resource utilization (ISRU) capabilities to the Presidents vision for space exploration, the National Aeronautics and Space Administration (NASA) identified the following objectives. First, identify and characterize resources on the Moon, especially the polar regions. Second, to demonstrate ISRU concepts, technologies, and hardware that reduce the mass, cost and risk of human endeavors to Mars. This includes excavation and material handling, volatile/hydrogen/water extraction, thermal and chemical processing for oxygen production, and cryogenic fluid storage and transfer. These four supporting objectives require

serious effort to successfully design and deploy such systems. Third, to gain operation experience and mission validation for Mars by pre-deployment and activation of ISRU assets, producing and transferring consumables from the lunar surface, landing a human crew with pre-positioned resources, and long mission durations. Fourth, to develop and evolve lunar ISRU capabilities that enable exploration abilities. This includes long range surface mobility with power rich distributed systems to enhance science by providing global access. Finally, to develop and evolve lunar ISRU capabilities to support sustained, cost efficient human space transportation and a human presence on the Moon.[2] Current NASA Administrator Mike Griffin remarked that "… the architecture can make significant use of lunar resources. At first, in all likelihood oxygen [will be] obtained by solar roasting", when he first introduced the Crew Exploration Vehicle that will be the vehicle to return humans to the Moon.[3]

Future augmentations to the space transport system include cheaper access to space through reusable transportation hardware, and by fostering relationships between government and commercial organizations. NASA plans to achieve these five objectives in four phases of operation: robotic, sortie, pre-deployment, and outpost. The robotic phase achieves identification and partial characterization of lunar resources with through data collected by the Lunar Reconnaissance Orbiter (LRO), and the Lunar Robotic Exploration Program's robotic probes to polar regions of interest (RLEP-2). The sortie phase of lunar exploration is the first phase to include humans. It is designed to validate systems and operations prior to the deployment of an outpost. Critical ISRU capabilities such as excavation, oxygen production, hydrogen extraction, cryofluid storage and transfer will be demonstrated to scale production rates. The pre-deployment phase uses full-scale ISRU systems to excavate regolith, extract useful volatiles (H_2, H_2O, CO, N_2), produce oxygen and fuel cell reagents, and store products in a cryogenic state. The outpost phase fully employs pre-positioned in situ resource utilization systems and upgrades the technology over time. The outpost initially uses a pilot plant sized to support refueling two ascent vehicles per year (3500 kg/vehicle) and habitat/EVA requirements for four crew members (~3000 kg). Mid-term outpost objectives are to achieve *in situ* fabrication and repair, power generation, thermal storage, and an improved oxygen production plant with larger production rates. Long term lunar capability objectives are to truly "live off the land"; constructing complex parts and habitats with in situ resources, provide life support, and possibly achieve helium 3 isotope collection.[2]

In the near term, the most easily exploitable resource is the lunar regolith. Lunar soil, or lunar regolith, is the outermost debris layer of the lunar surface. Lunar regolith is unaffected by an atmosphere, water, life, or recent geological activity. It's shaping has occurred by micrometeorites pulverizing lunar rocks over billions of years into a fine powder. Impact glasses, volcanic glasses, agglutinates, mineral fragments, and rock chips form the makeup of lunar regolith[3]. Unlike the Earth, the Moon lacks organic materials in its chemistry, but has similar minerals, basalts, and agglutinates as on earth. The lunar regolith is composed of mainly silicate and other oxide minerals, both containing oxygen. By mass percentage, the lunar regolith is approximately forty percent oxygen. Lunar regolith composition will be discussed in section IV. Liberating this oxygen to be condensed, stored, and later used, is the goal of studies involving *in situ* production of oxygen from lunar regolith.

Multiple methods of lunar oxygen extraction have been introduced; many have been investigated, but few have been tested to a high level of technology readiness. Extraction techniques can be classified by five descriptive categories: gas-solid, gas-liquid, bulk electrolysis, pyrolysis, and slurry-solution. Gas solid interactions generally have the highest level of technology readiness. Ilmenite reduction by hydrogen is currently at a technology readiness level of 4, where validation and demonstration of the concept in a laboratory environment has been completed. Ilmenite reduction has been thoroughly tested on lunar simulants and on Apollo return samples, achieving oxygen production at approximately 1.5 percent efficiency.[4] Technology Readiness Levels (TRL) are a systematic measurement system that supports assessments of the maturity of a particular technology and the consistent comparison of maturity between different types of technology.[5]

TRL 1	Basic principles observed and reported
TRL 2	Technology concept and/or application formulated
TRL 3	Analytical and experimental critical function and/or characteristic proof-of concept
TRL 4	Component and/or breadboard validation in laboratory environment
TRL 5	Component and/or breadboard validation in relevant environment
TRL 6	System/subsystem model or prototype demonstration in a relevant environment (ground or space)
TRL 7	System prototype demonstration in a space environment
TRL 8	Actual system completed and "flight qualified" through test and demonstration (ground or space)
TRL 9	Actual system "flight proven" through successful mission operations

Pyrolysis is a form of incineration that decomposes materials through heat in the absence of oxygen, in this case in vacuum. Solar vacuum pyrolysis takes advantage of the abundant energy available through solar radiation to heat material in a vacuum, where convection losses are eliminated. Once heated above a material's vaporization temperature, the molecules begin to dissociate into monoxides, metals, and oxygen. While cations and anions are present, the sample is rapidly quenched below the condensation temperature of the monoxides and metals, thus releasing gaseous oxygen. No consumables are needed in the reaction, any type of lunar regolith can be used without beneficiation as a feedstock, and no catalysts are required. Beneficiation is the term used to designate the processing of an ore to concentrate a particularly useful mineral or element. This process is characterized by its total reliance on space resources, namely a high vacuum and solar energy. It allows mission planners to employ the strategy of "living off the land" when higher efficiencies are required. Vacuum reduction and distillation of metals are well-known terrestrial processes.[6]

Literature Review

The prospect of *in situ* resource utilization, specifically the production of oxygen, has been studied since the Apollo era. The technique of vacuum pyrolysis was first introduced by Stuerer and Nerad in 1983. Steurer provided conceptual arguments for thermal dissociation and rapid condensation to produce oxygen. Steurer estimated that the gas flow path and flow rate should be maintained at an optimum level by control of the pressure differential between the vaporization region and the oxygen collection system with the aid of the environmental vacuum. It was also estimated that the energy required for vaporization and dissociation of the entire throughput is 5100 kWhr/ton.[7]

Constance Senior conducted solar furnace experiments with ilmenite and anorthite. Her experiments measured the pressure increase in a closed chamber during heating. A solar flux of 80 W was applied to the mineral samples. Corrections were made to the temperature and background pressure. Both materials showed a net pressure increase with time. The experiments confirmed thermodynamic equilibrium calculations that ilmenite showed a larger pressure increase than anorthite. The measured mass loss was consistent with the loss of oxygen by reduction of iron in the liquid phase. It was concluded that the pyrolysis of bulk lunar regolith is feasible for the production of oxygen in low-pressure environments and temperatures in the range of 2000 to 2500K.[8]

This study improves upon the experiments done previously by using a wider array of regolith simulants, increasing system power, increasing system instrumentation, and performing analysis on the evolved gases and reduced samples.

III. Objective

Goal

The goal of the lunar oxygen research project described here is to achieve oxygen production from bulk lunar regolith simulants through vacuum pyrolysis and apply the relationships from experimental tests to missions by scaling.

Metrics

Metrics for oxygen production are based on the requirements for both life support and propellant production. The metrics listed in Figure 2 below describe the oxygen requirement to be produced for life support. A goal of 5.5 metric ton O_2/year was derived from the centennial challenge issued by NASA in the spring of 2005.

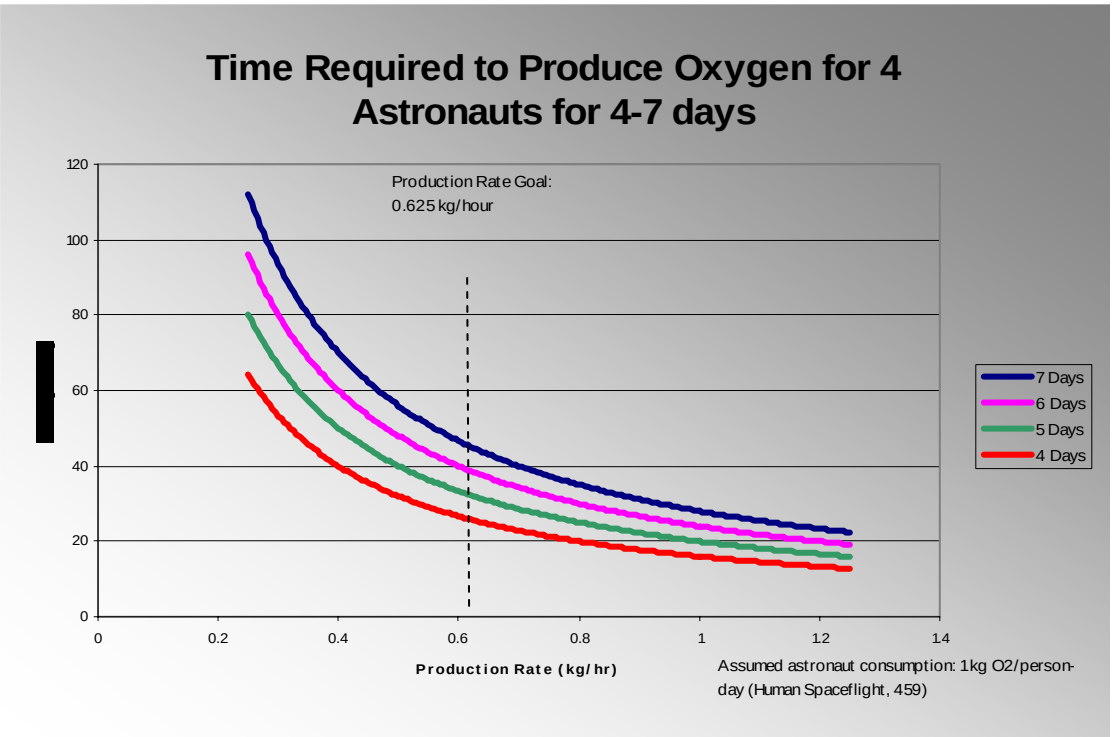

Figure 1 - Production Metrics for Life Support Oxygen[9]

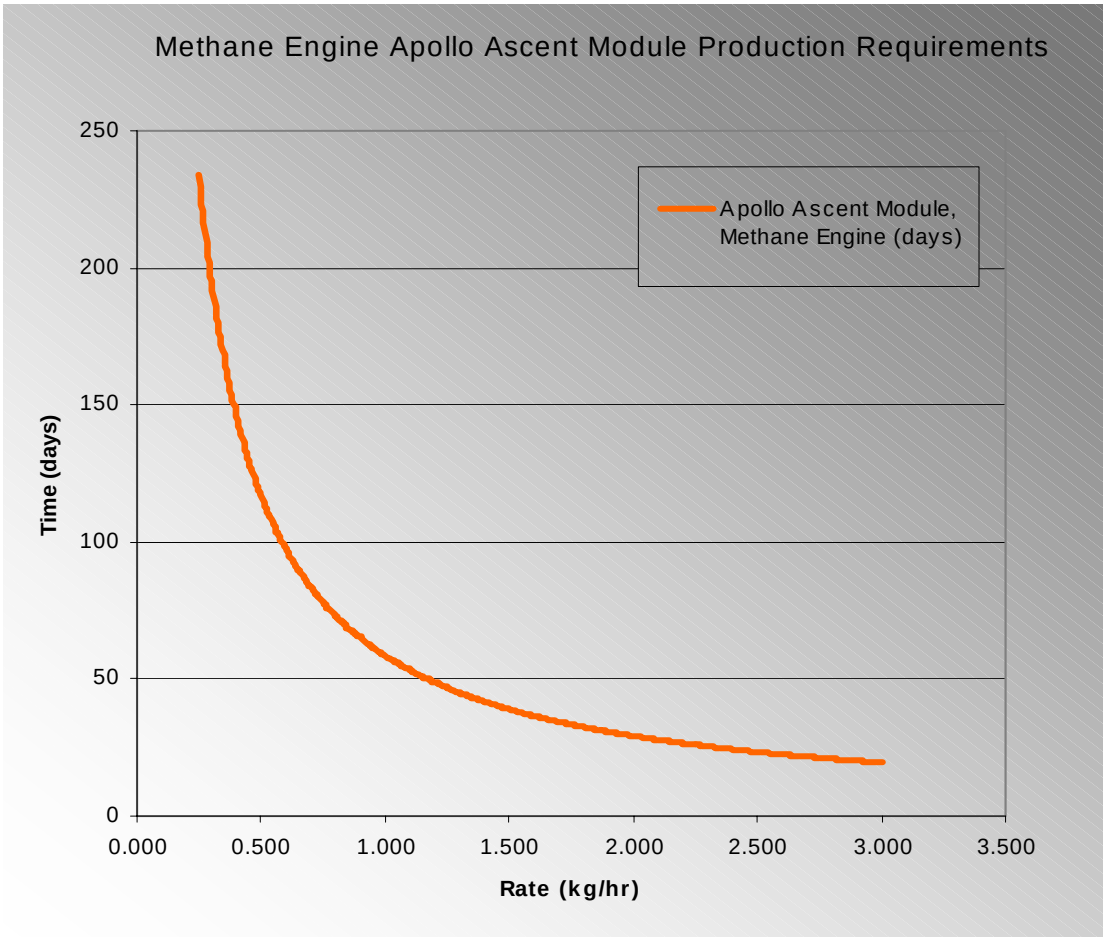

Figure 2 - Production Metrics for Propellant Production[9]

Figure 2 represents the requirements of an oxygen-methane lunar ascent engine. Methane engines with an oxidizer to fuel ration of 4:1 require an estimate 1400 kgs of oxidizer to perform the lunar ascent stage mission. Propulsion requirements estimated by Eagle Engineering during the design study of a lunar oxygen pilot plant determined that eight metric tons of oxygen per year is required. A full scale oxygen production plant capable of 1000 metric tons of liquid oxygen per year is needed to successfully augment a lunar space transportation system[9]. Support of the Crew Exploration Vehicle (CEV) mission architecture for two lunar ascents per year and life support for four astronauts requires production of 10 metric tons of oxygen per year.[2]

IV. Lunar Regolith

Formation and Properties

Lunar regolith is formed from lithic sources through meteorite-induced comminution and constructive processes of agglutinate formation and vapor deposition show in Figure 3 below.[11] The same impacts have mixed the soil vertically several meters and laterally over several kilometers. Lunar rocks are generally basalts, anorthosites, and breccias. Common minerals found in lunar regolith are olivine, pyroxene, plagioclase and feldspar. Agglutinates are composted of aggregates of bonded rock and mineral, altered by impact material and solar wind, forming a glass.[12] Oxygen is present as the negatively charged anion linked in complicated networks to cations (Si, Al, Mg, Ti, Fe) in the crystal structure of a lunar mineral.

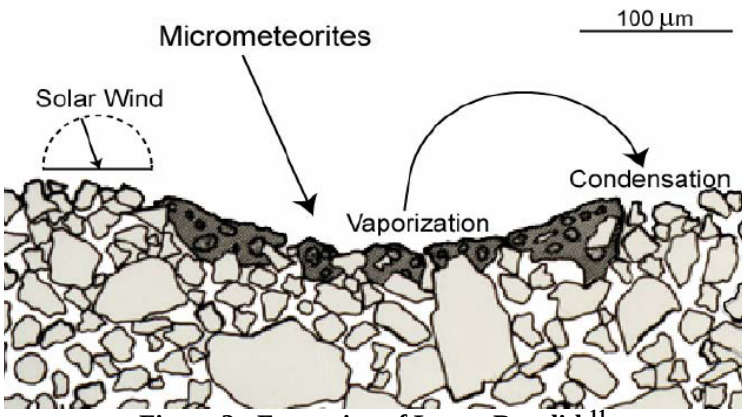

Figure 3 - Formation of Lunar Regolith[11]

Both lunar and terrestrial rocks are made up of minerals. A mineral is defined as a solid chemical compound that (1) occurs naturally; (2) has a definite chemical composition that varies either not at all, or within a specific range; (3) has a definite ordered arrangement of atoms; and (4) can be mechanically separated from the other minerals in the rock. Glasses are solids that may have compositions similar to minerals, but they lack the ordered internal arrangement of atoms. Lunar minerals may have a specific unvarying composition like quartz (SiO_2), but most have a composition that varies in a regular manner between two or more endmember components. Over ninety percent of lunar rocks by volume are silicate minerals, most commonly pyroxene $(Ca,Fe,Mg)_2Si_2O_6$, plagioclase feldspar $(Ca,Na)(Al,Si)_4O_8$, and olivine $(Mg,Fe)_2SiO_4$. Oxide minerals, including ilmenite $(Fe,Mg)TiO_3$ and spinel, are next in abundance after silicate minerals. Spinels contain other metals such as chromium, aluminum, and iron. Soil compositions contain rock fragments, minerals and agglutinates shown below in Figure 4. [12]

Lunar Regolith has a median particle size from 40 to 130 μm, with the mean being 70 μm.[12] The unique and complex nature of lunar soil has been imposed largely by the presence of abundant agglutinates, nearly fifty percent. The erratic character of agglutinates makes it very difficult for terrestrial analogues to simulate a lunar environment.

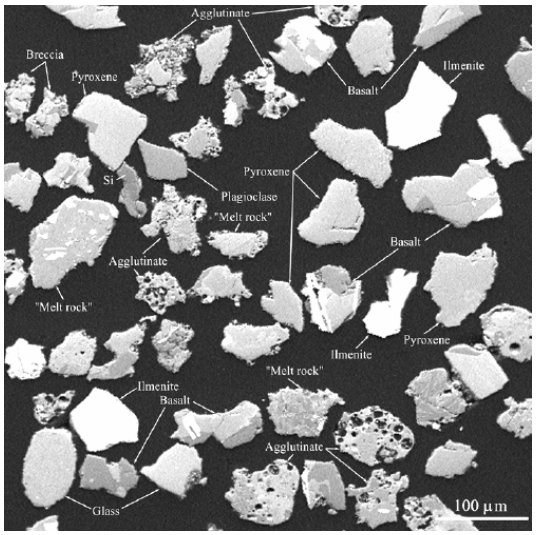

Figure 4 - Regolith makeup including agglutinates, rock chips, impact glasses, volcanic glasses, and plagioclase[11]

This study simulates lunar regolith with geological minerals that are similar to lunar minerals. The silicate mineral pyroxene is simulated with terrestrial enstatite $MgSiO_3$. Terrestrial ilmenite is used to simulate oxide minerals. The mare simulant, MLS-1a is used to represent the chemical composition of lunar regolith. MLS-1a is a terrestrial representation of Mare Tranquilitatis regolith chemistry. Since each simulant composition is different, the dissociation behavior is expected to be different. The chemical composition of various lunar landing sites by the Apollo and Luna missions are shown below in Figure 5. The majority of the regolith is silicon dioxide, aluminum oxide, iron oxide, magnesium oxide, and calcium oxide. The remaining oxides form minor components of lunar regolith.

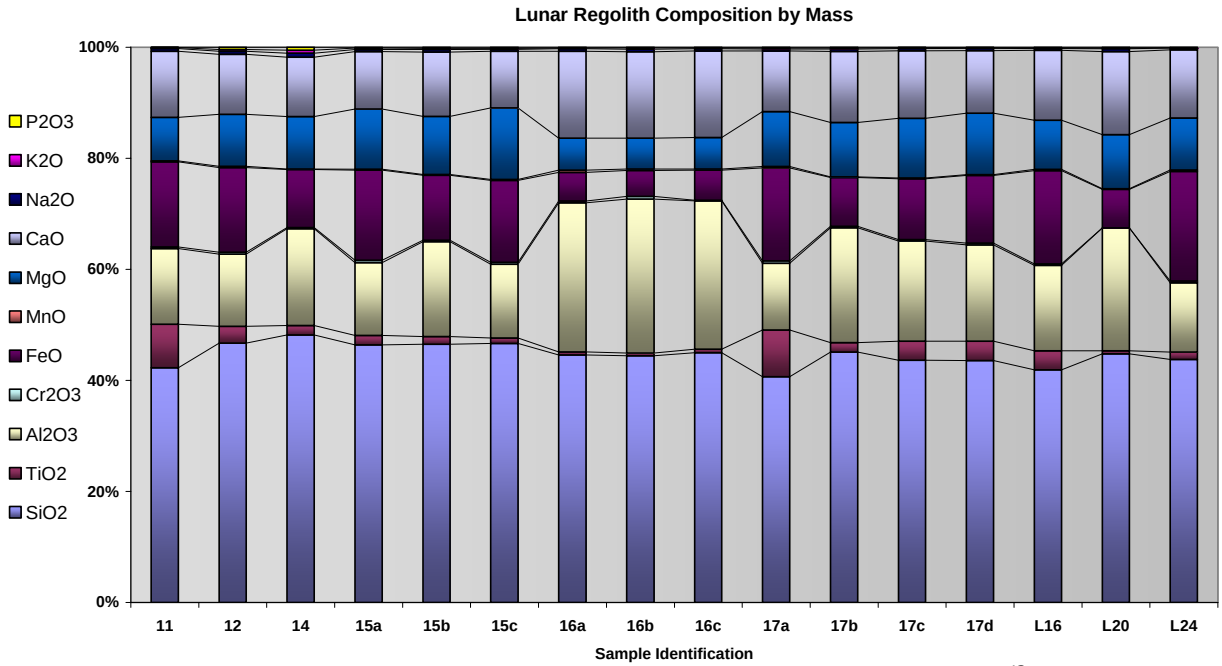

Figure 5 - Apollo and Luna Mission Lunar Sample Composition by Mass[12]

Lunar Regolith Volatiles: Hydrogen, Carbon, Nitrogen, Sulfur, Fluorine, Chlorine

Solar wind consists of energetically charged particles that flow radially outward from the solar corona. The solar wind is deflected by magnetic fields but absorbed by surface materials on a body like the Moon. Solar wind is predominantly hydrogen and helium, with the abundance of heavier elements decreasing with increasing atomic mass. Table 1 below summarizes volatile species found at Apollo sites. Trace elements hydrogen, carbon and nitrogen are present in the regolith from solar wind.[5] Solar wind only penetrates a few micrometers into the absorbing agglutinates and minerals of lunar regolith. These elements are considered lunar volatiles because they easily vaporize at low pressures found on the Moon. Solar wind derived volatiles are concentrated in the finest grain sizes, where the surface to volume ratio is largest. [5] Volatiles are important because they may provide necessary elements for the survival of a lunar outpost. At 700°C near quantitative release of hydrogen and helium will occur while 20 – 30% of the nitrogen and carbon will co-release.[13]

Solar Wind Implanted Volatiles in Apollo Regolith

	Hydrogen	Helium	Carbon	Nitrogen
Apollo 11	20 - 100	20 – 84	96 - 216	45 – 110
Apollo 12	2 - 106	14 – 68	23 – 170	46 – 140
Apollo 14	67 - 105	5 – 16	42 – 225	25 – 130
Apollo 15	13 – 125	5 – 19	21 – 186	33 – 135
Apollo 16	4 – 146	3 – 36	31 – 280	4 – 209
Apollo 17	0.1 - 206	13 - 41	4 - 200	7 - 94
Temperature of Release (°C)	200 – 700 °C	200 – 700 °C	CO_2: 200 – 600 CO: 600 – 1200	700 – 900 °C 1000 - 1200 °C

Table 1 - Concentration of Solar Wind Implanted Volatile Species (Parts per Million)[13]

V. Technique

Experimental work on the vacuum pyrolysis method was completed at the Goddard Space Flight Center in Greenbelt, Maryland. The experimental setup shown below in Figure 6 draws solar energy through a focused Fresnel lens into a vacuum chamber where the lunar regolith simulant is located within a crucible. The vacuum pyrolysis technique, also referred to as vapor phase reduction, is dependent on four main factors: the solar energy transfer into the system, the dissociation of the regolith into monoxides, metals, and oxygen, the condenser properties of the system, and the characteristics of the experimental setup. These factors are discussed in the following sections.

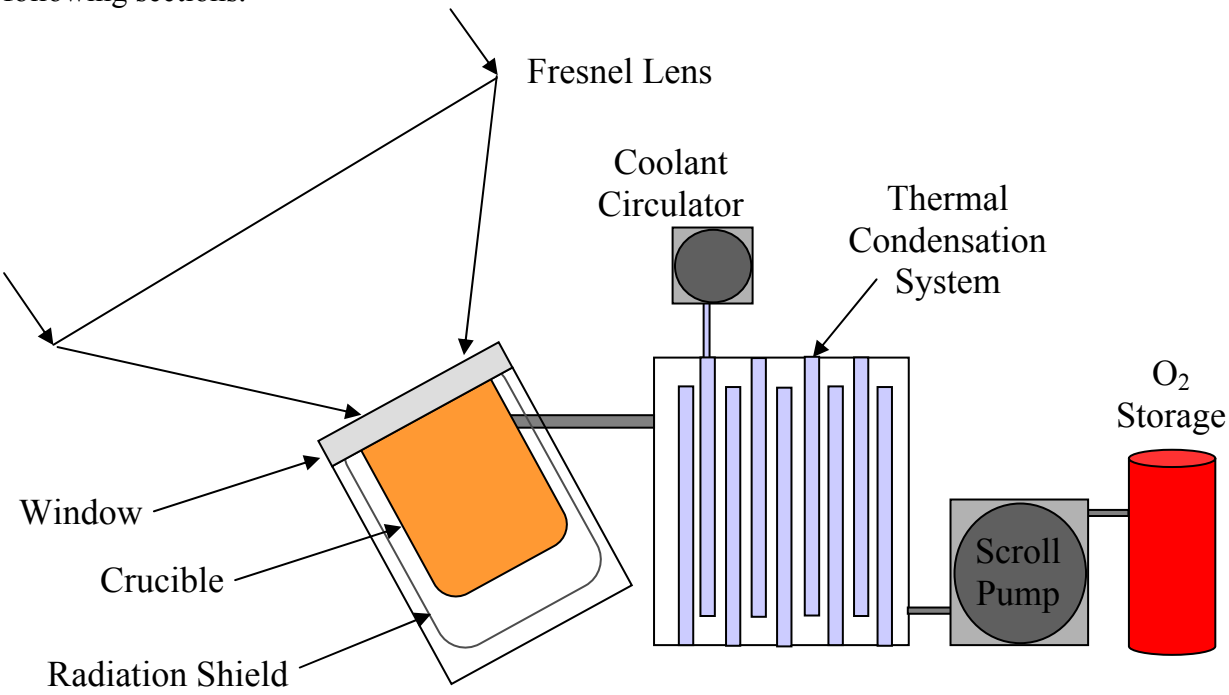

Figure 6 - Pyrolysis Experimental Setup with Fresnel lens[4]

Solar Energy Transfer

The energy required to achieve molecular dissociation in vacuum pyrolysis is supplied by solar photons. An operational lunar vacuum pyrolysis production plant would have a solar path including the Fresnel lens, vacuum chamber window, and the regolith itself. Due to the lack of atmosphere on the Moon, the Moon experiences an average solar flux approximately equal to the solar constant, 1373 watts per square meter. There is a lunar day cycle that provides continuous flux for fourteen days, followed by darkness for fourteen days. There are latitudes which maximize solar exposure, which include the poles. The power transmitted by solar radiation is distributed unevenly across the spectra. Figure 7 represents the solar spectral irradiance at varying wavelengths of light.

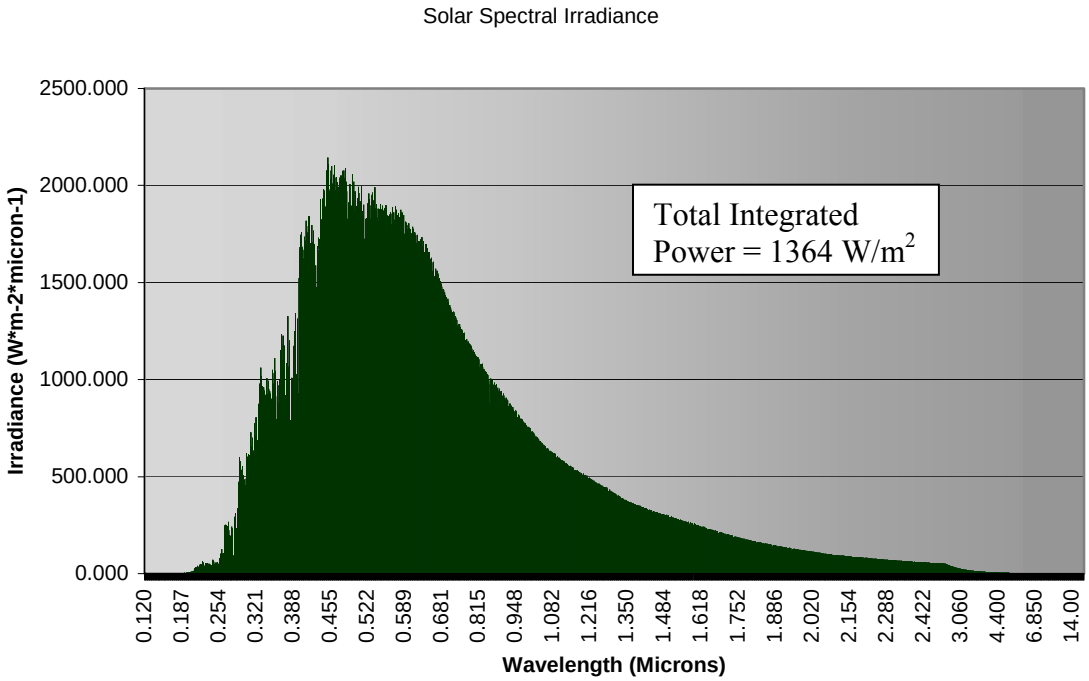

Figure 7 - ASTM E490 solar spectral irradiance[14]

For engineering purposes, it is critical to minimize transmission losses in the system. It is desirable to exploit as much energy as possible provided by the sun for pyrolysis and avoid heating system components. Pyrolysis is the most energy intensive process of those capable of oxygen production.[1] Either transmission losses must be minimized or the solar concentrator must increase in area to increase system power. A possible challenge will be to minimize dust coatings that were frequently noticed in the Apollo program. Dust will reduce the spectral transmission by absorption and scattering.

In terrestrial experiments, lunar simulants do not receive the same solar irradiance as lunar regolith would on the surface of the Moon because of partial spectral absorption in the Earth's atmosphere. Terrestrial spectral transmittance is represented in Figure 8. Direct scaling is not appropriate when comparing the power requirements of a lunar terrestrial system.

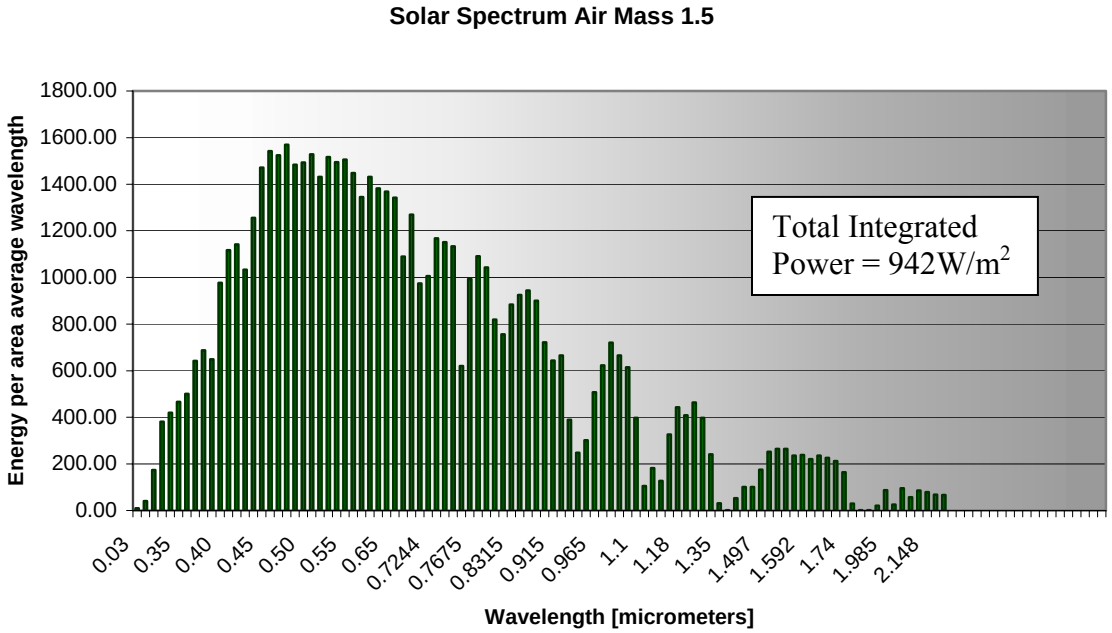

Figure 8 - US standard atmosphere with rural aerosol model[15]

There is a significant drop in integrated power, about 400 watts per square meter or 30% between terrestrial and lunar solar spectrums. Much of the power is lost in absorbed ultraviolet light by the upper atmosphere. The solar spectrum standard in Figure 8 represents the average conditions in the 48 contiguous states of the United States. It includes the irradiance distribution of solar radiation through an air mass directly and diffusely. Comparing Figure 7 and Figure 8 shows varying irradiances at similar bands of light. Therefore, simple scaling of terrestrial experiments to an engineering design for an operational lunar system will mischaracterize the actual lunar system's behavior.

The third major transmission loss is through the focusing medium. These experiments used a polymer-formed Fresnel lens, just over one square meter in area. The spectral transmission from the sun, through the atmosphere and through the Fresnel lens is depicted in Figure 9. This provides an initial estimate of the power supplied to the regolith simulant.

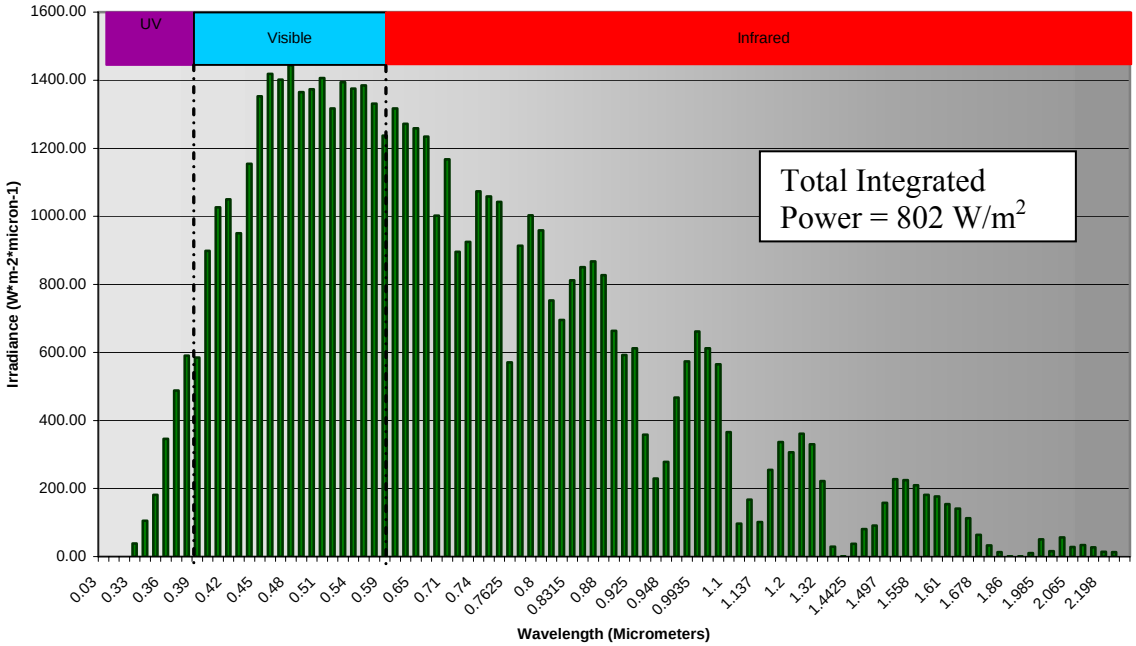

Figure 9 - Fresnel lens transmitted spectral irradiance[15]

Fifteen percent of the solar energy passing into the Fresnel concentrator is lost from absorption, reflection, and scattering associated with the lens. Other loss mechanisms include losses produced from the vacuum chamber window and the absorption characteristics of the regolith. The lunar sourcebook provides reflectance data for various mare and highlands regolith collected during the Apollo missions. Mare soil, being less mature than highlands soil, is darker, thus absorbing more light. Mare soil reflectance accounts for an eighteen percent loss between the total energy transmitted and total energy absorbed, while highland regolith reflects twenty percent of solar energy. All pyrolysis tests described in this report were done using vacuum flange fittings with glass windows, unless otherwise noted. The glass accounts for an eight percent loss in solar energy transmission. The glass transmission ratio for the vacuum window and regolith reflectance relationships are shown below in Figure 10.

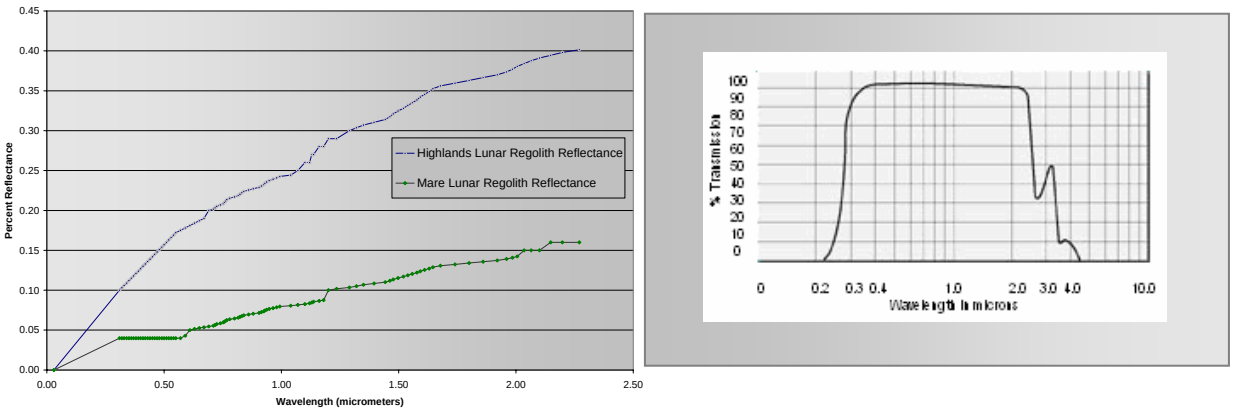

Figure 10 - Reflectance Spectral Properties of Lunar Soil[12] and Vacuum Window Transmission[16]

The optical path, from source to the crucible, experiences losses from atmosphere, concentrator, vacuum window, and the absorbance characteristics of the sample. Assuming a sunny day with low humidity modeled according to the standard E 490[15] with a polymer fresnel lens and a glass window, approximately 610 watts is available for pyrolysis of the regolith. This data is restrictive to terrestrial based experiments as the solar standard E 490 is employed to model solar transmission to areas in the United States. On the surface of the Moon with no atmospheric attenuation, approximately 800 watts is available for pyrolysis. The reflectance properties of regolith are fixed, but better concentrating devices and vacuum lenses can provide larger work potentials for pyrolysis on regolith for increased oxygen production efficiency.

Vaporization and Dissociation

Once regolith is heated to a vapor, additional heating causes its oxides to dissociate into suboxides and free oxygen. The heating breaks molecular bonds modeled by the Gibbs free energy equation:

$$G = H - T \cdot S,$$

where 'G' is Gibbs free energy, 'H' refers to enthalpy, 'T' is temperature, and 'S' refers to entropy. The Gibbs equation is needed to compare and model the mutual stability of individual suboxides, oxygen and metals. The dissociation process is dependent on both temperature and pressure. Lower pressures reduce the energy needed for free radicals to escape. Therefore, to achieve maximum oxygen production, a pyrolysis system requires high chamber temperatures and low pressures. A balance must be established between pressure and temperature to achieve optimal conditions for oxygen production since pressure increases with increased temperature. This balance depends on the volume of the pyrolysis chamber, the energy flux, and the amount of regolith in the reaction. In multicomponent mixtures, the total Gibbs free energy is the sum of the free energies for all coexisting phases[17]:

$$G = G_{gas} + G_{liquid} + G_{solid}$$

As described previously, nearly all of lunar materials are oxides, making oxygen forty percent of lunar surface materials by weight. The dissociations follow a simple relationship of *Oxide + Heat → reduced oxide (g) + ½O_2 (g)*. The most common dissociation relations, ordered by average concentration, present when lunar regolith is heated to elevated temperatures are shown below in Table 2. Minority oxides, less than one percent of regolith composition, were not included in the dissociation process because they provide at least an order of magnitude less oxygen than the major oxides.

Dissociation Equations	Bond Dissociation Energy at 0 K (kJ/mol)	Vaporization Temperature at 10^{-3} atm (K)	Free Energy (kJ/mol) 398K
SiO_2 + Heat → SiO (g) + ½O_2 (g)	707.6	1973	-302.1
Al_2O_3 + Heat → Al_2O_2 (g) + ½O_2 (g)	1030	2740	-1582.3
FeO + Heat → Fe (g) + ½O_2 (g)	410.3	2300	-244.1
CaO + Heat → Ca (g) + ½O_2 (g)	431.3	2650	-603.3
MgO + Heat → Mg (g) + ½O_2 (g)	418.7	2450	-569.3
TiO_2 + Heat → TiO (g) + ½O_2 (g)	669.9	2275	-888.8

Table 2 - Dissociation of the Oxides[18,19]

Since regolith contains many combinations of oxides within its agglutinates, minerals and rock fragments, oxides will not always dissociate according to the simplified equations present in Table 2. To gain an understanding of the complex interplay of multiple oxide behavior, the HSC Chemistry 5.11 computer program was employed to model how each solid metal oxide breaks into constituent parts as temperature is increased.[20] The HSC software was validated by comparing its results with CL Seniors published equilibrium calculations for ilmenite.[8] This program assumes that pressure is held constant at 10^{-4} bars within the chamber during dissociation ('A' labeled graphs in Figures 10 - 16). The program maximizes the Gibbs free energy equation to determine the equilibrium composition at each temperature. A comparison is made between experimental pressures and lunar pressures. The Moon provides a much lower ambient pressure, allowing chamber pressures to become very low without large pumping mechanism. It is assumed that the chamber pressure for lunar operations is 10^{-10} bar ('B' labeled graphs). The ordinate for each dissociation relationship represents equilibrium composition in kilograms, while the abscissa is the temperature in degrees Celsius. The relationship between vaporization temperature and pressure is not fully known, but it is known that vaporization temperature for a substance increases with an increase in pressure. The graph below in Figure 11 shows the dissociation relationship between temperature and pressure for mare regolith. Equilibrium calculations show that there is an exponential relationship between temperature and pressure.

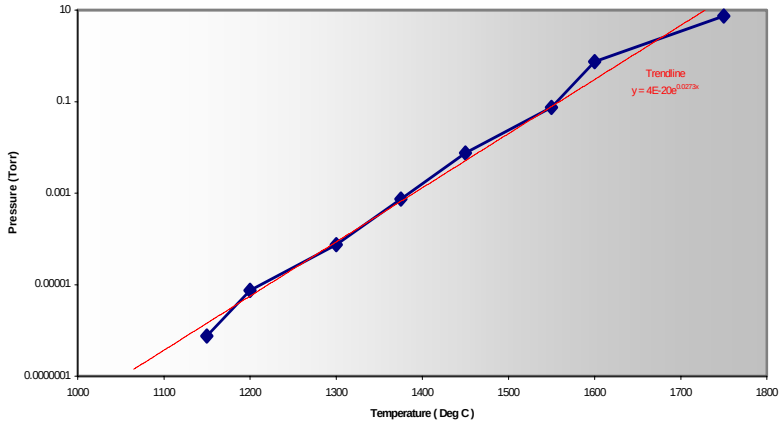

Figure 11 – Mare Regolith Dissociation Relationship between Temperature and Pressure

Silicon Dioxide

Silicon dioxide forms two main oxides: SiO and SiO_2. The main partial pressure components in equilibrium in the gas phase are silicon monoxide and molecular oxygen.[21] It begins to vaporize at 1800 ^oC at a pressure of 10^{-4} bar and 1100 ^oC at 10^{-10} bar. The maximum amount of recoverable oxygen is available at 1840 ^oC and 1180 ^oC respectfully. The proportion of atomic oxygen will continue to increase as it remains the only form of oxygen present at very high temperatures. Atomic oxygen readily oxidizes any surface that it strikes. It is important to target temperatures that maximize O_2 production, and to avoid increasing the system temperature where O_2 dissociates. O atoms are more likely to oxidize the system's metallic hardware than it is to combine with another O atom to form gaseous oxygen. The metallic hardware will react to form an impermeable oxide layer. This will occur during commissioning, where monatomic oxygen is not more likely to react with other gases than solid surfaces. At temperatures above 1425^oC, the partial pressure of oxygen is greater than the partial pressure of silicon monoxide.[21] SiO_2 has a theoretical yield of 0.27 g O_2 produced for every gram dissociated[17].

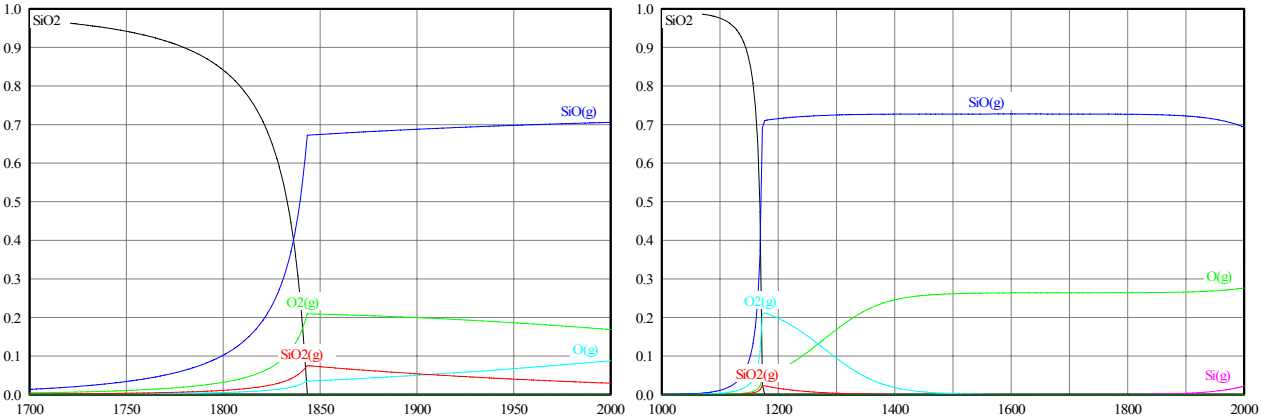

[A] Temperature (^oC) [B]

Figure 12 - Dissociation of Silicon Dioxide at 10^{-4} and 10^{-10} bars

Aluminum Oxide

The most important and the most stable aluminum oxide is alumina, Al_2O_3. Since Al_2O_3 has larger bond dissociation energy, it vaporizes and dissociates at higher temperatures than silicon dioxide at comparable chamber pressures. The species AlO, Al_2O, and Al_2O_2 have been noted in the gaseous phase. The main components of the gas phase over aluminum oxides throughout the temperature range between 700^oC to the boiling point are monatomic gases, oxygen and aluminum. With the increase in temperature, the concentration of the suboxides Al_2O and AlO increase, reaching 10% at 2700 ^oC, the majority being gashouse oxygen and aluminum.[21] Aluminum oxide begins to vaporize at 2200 ^oC at a pressure of 10^{-4} bar and 1410 ^oC at 10^{-10} bar. The maximum amount of recoverable oxygen is available at 2340 ^oC and 1475 ^oC respectively. Aluminum oxide has the largest vaporization temperature for all of the regolith oxides. Al_2O_3 has a theoretical yield of 0.31 g O_2 produced for every gram dissociated[17].

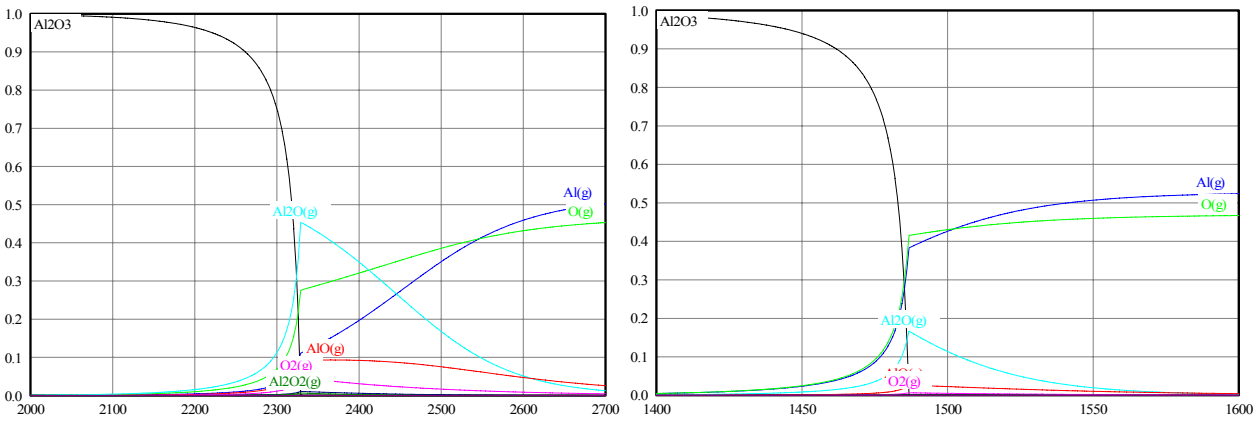

[A] Temperature (^{o}C) [B]

Figure 13 - Dissociation of Aluminum Oxide at 10^{-4} and 10^{-10} bars

Iron Oxide

Sources in gas dynamics contain contradictions of the behavior of the dissociation of iron oxide. Thermodynamicists Brewer and Kulikov conclude that all ferrous oxides will dissociate when the thermal conditions are appropriate, and provide data of vaporization and dissociation, but Shrunk suggests that FeO does not dissociate at all. The nature of iron oxides is exceedingly complex. In the liquid state, iron oxides contain more oxygen than would correspond to the stoichimetric formula FeO.[21] According to this computer model, iron oxide begins to vaporize exponentially at 1800 ^{o}C, at a pressure of 10^{-4} bar and 1000 ^{o}C at 10^{-10} bar. Since iron oxide only contains one oxygen atom, very little gaseous O_2 occurs naturally. Iron oxide will assist the overall production of oxygen from lunar regolith because oxygen released from iron oxide will interact with other free radicals in the regolith. This will eventually dissociate and recombine to form O_2. Iron oxide has the lowest value of free energy, making it easier to obtain oxygen from iron than other metals in lunar regolith. FeO has a theoretical yield of 0.22 g O_2 produced for every gram dissociated when reacted on its own[17].

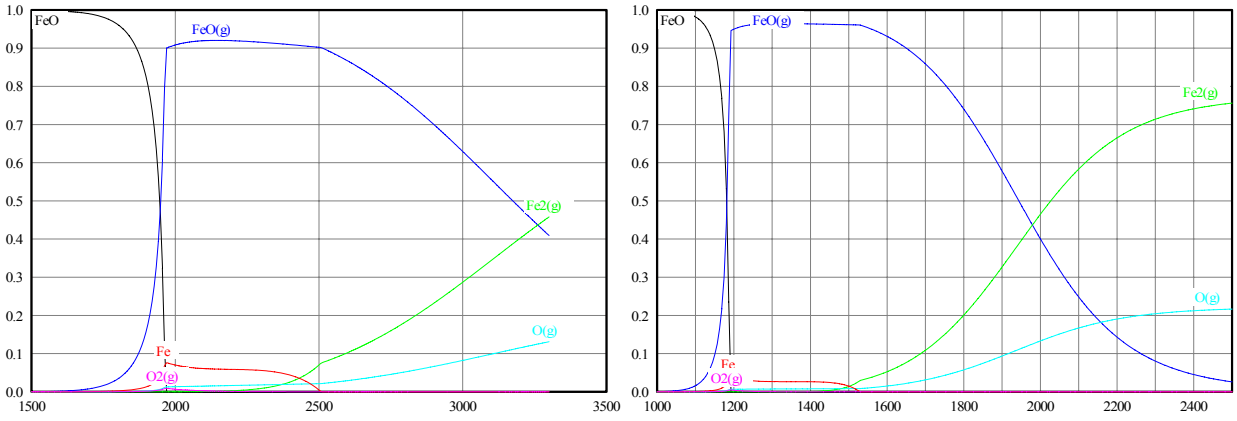

[A] Temperature (^{o}C) [B]

Figure 14 - Dissociation of Iron Oxide at 10^{-4} and 10^{-10} bars

Calcium Oxide

Calcium oxide slowly changes state when heated to a liquid, then at 2100°C and 10^{-4} bar, it vaporizes and dissociates. Calcium oxide begins to vaporize at 1250°C and 10^{-10} bar. Similar to iron oxide, calcium oxide contains only one oxygen, so the O_2 yield is smaller than dioxide molecules. Calcium oxide has the third largest bond energy and third largest free energy compared with the other major oxides. CaO has a theoretical yield of 0.29 g O_2 produced for every gram dissociated[17].

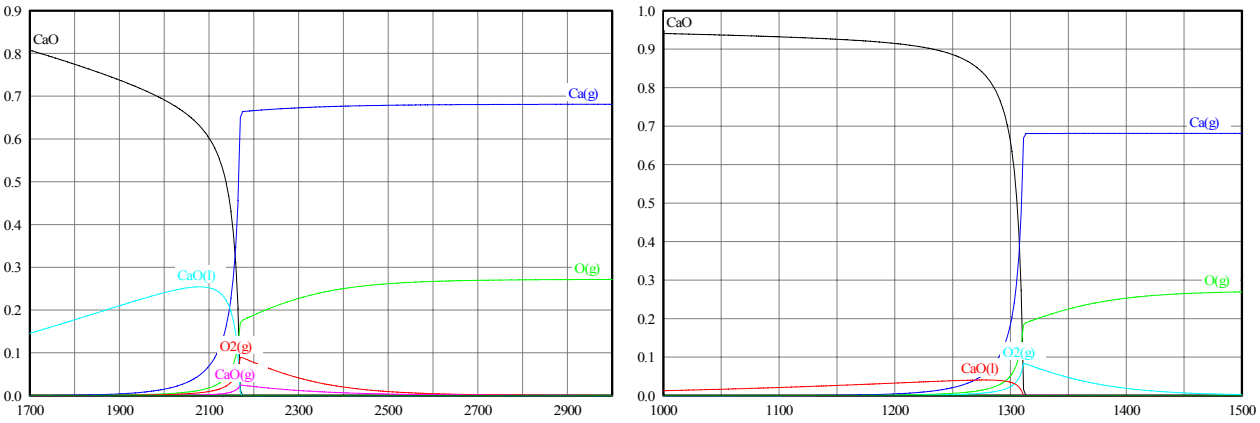

Figure 15 - Dissociation of Calcium Oxide at 10^{-4} and 10^{-10} bars

Magnesium Oxide

Magnesium oxide vaporizes and dissociates at high temperatures for a diatomic molecule. Only calcium oxide requires more energy to break the metal to oxygen bond. Gaseous oxygen is produced at 1900 °C and 1180 °C at 10^{-4} and 10^{-10} bar respectively. This dissociation and recombination is unique because it is possible to obtain a thirty percent yield on O_2 if the process is efficient. MgO has a theoretical yield of 0.29 g O_2 produced for every gram dissociated.

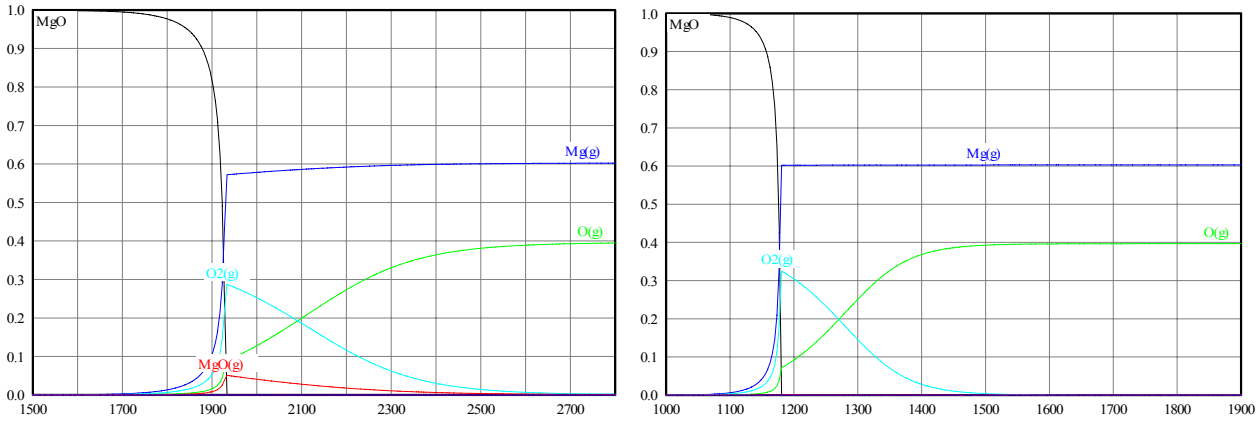

Figure 16 - Dissociation of Magnesium Oxide at 10^{-4} and 10^{-10} bars

Titanium Dioxide

Titanium forms a number of oxides: TiO_2, Ti_3O_5, Ti_2O_3, and TiO. Titanium oxide is commonly found as ilmenite ($FeTiO_3$) in regolith, having unique dissociation behavior. Very little O_2

occurs, but monatomic oxygen is present at higher temperatures. According to Kulikov, the partial pressure of O_2 greatly increases as temperature increases. His calculations conclusions were based on equilibrium calculations, not validated trough direct experimental results. It is this high yield of atomic oxygen that can recombine with other oxygen atoms to form gaseous O_2.

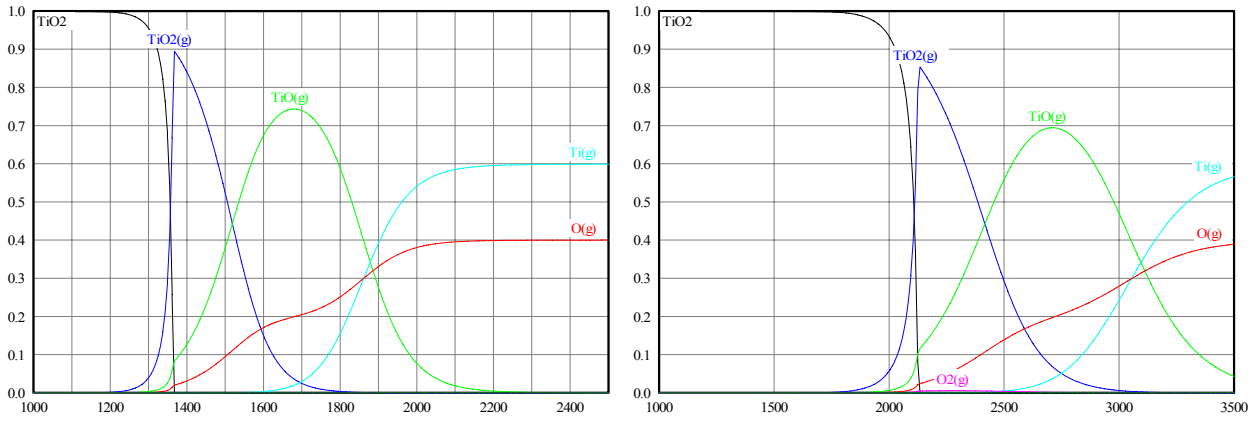

Figure 17 - Dissociation of Titanium Oxide at 10^{-4} and 10^{-10} bars

The dissociation of lunar regolith contains all of the previous individual dissociations as well as the dissociation of the minority oxides [MnO, Cr_2O_3, K_2O, P_2O_3, Na_2O]. A comparison shows that lower temperatures are needed to extract oxygen from silicon, magnesium and iron than calcium and aluminum. It is necessary to carry out equilibrium calculations for the entire composition of lunar regolith to understand what temperature maximizes oxygen yield from the combination of all oxide dissociation. If the temperature continues to increase, oxygen dissociates into atomic oxygen. Atomic oxygen reacts with nearly any surface it strikes. It is therefore necessary to maximize the concentration of O_2 in the equilibrium compositions, and tailor the pyrolysis system to operate at this temperature. The equilibrium components are shown below as concentration versus temperature in degrees Celsius. This equilibrium dissociation relationship is modeled after the average composition of all Apollo 15 samples.

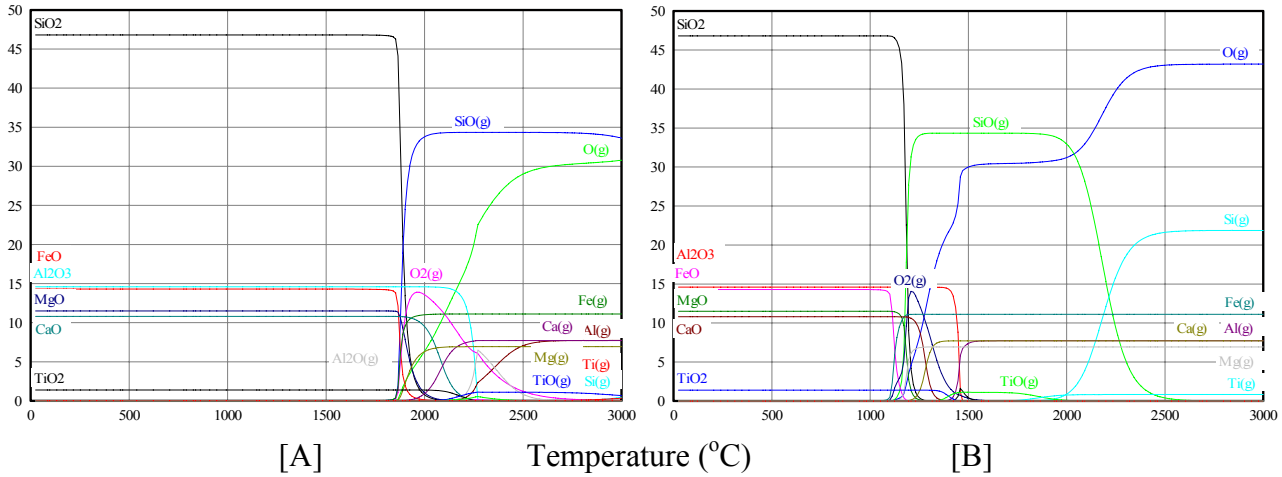

Figure 18 - Apollo 15 average regolith percentage composition dissocation behavior and temperature maximizing O_2 production.

Observing the dissociation and recombination behavior of multiple oxides shows an oxygen yield between ten and fifteen percent at both medium and high vacuums. This yield translates into maximum oxygen efficiency if the condensation system is completely effective. The most efficient operating temperature for maximum oxygen production is between 1800-2100 ^{o}C at rough vacuum and between 1300-1400 ^{o}C at high vacuum. It is also important to note the amount of regolith fully vaporized in the dissociation process. It is unlikely that less than all of the regolith will fully vaporize in this process. Partial vaporization will result in a decrease of system efficiency.

Thermal Distillation and Condensation

The largest technical challenge in the pyrolysis system is the selective condensation of regolith vapors to achieve maximum oxygen production. This is accomplished by establishing a gas flow through a thermal gradient. The dissociated regolith vapors are pulled from the pyrolysis chamber by a vacuum pump into a decreasing temperature gradient. Controlling the temperature of the condensing gradient is critical as it must transfer energy of condensation away from the surface material. The condensing surface must maintain a temperature below the lowest condensing temperature of reduced oxide/metal, but the temperature must not be too low. The sticking coefficient of oxygen decreases with increasing surface temperature. [17] The surface temperature must be high enough to reduce the residence time of the oxygen on the surface. Condensation of metal containing species without oxidation is the key to good oxygen yields. The temperature of the condensing surface determines the degree of oxidation of the deposit. This study investigates the temperature range and condensation distance where oxygen production is maximized.

The condensation system must also remove the reduced oxides and metal "slag" from the system on a continuous or batched basis. The removal of waste products poses an engineering challenge. Nothing less than complete vaporization of lunar regolith will leave some amount of substance in the crucible. If the crucible is to be reused, it must be cleaned. There must be the introduction of another fluid, mechanical scraping, removal of the crucible, or shaping the crucible to take advantage of lunar gravity.

Both the condensation chamber and pyrolysis chamber will use gravity in its design so that the slag slowly drips to a collection pan. The slag can then transported or stored. Prototype designs may decide to collect slag at the bottom of the chamber to be removed when the pilot plant is not in operation. A potential secondary use for the pyrolysis technique is the ability to cast slag into various shapes and objects. This may provide structure and radiation shielding for outpost construction. Potential byproducts of the pyrolysis process include high temperature refractory glasses, ceramics, and metals. Materials can be identified for selective removal by thermal distillation. It may be possible to use the reduced oxides present in the slag as high temperature crucibles in future operations.

Once the slag is removed from the product gas stream, impurities may still be present. The oxygen gas will need further fractional distillation and filtration before the *in situ* resource may be employed in life support and propulsion systems. Finally, the gaseous oxygen is cooled and

compressed in a cryocooler to be stored in its liquid form. This provides a storable and transportable fluid that can easily integrate into a life support, propulsion or fuel cell system.

Experimental Setup

The experimental system was required to be very flexible to provide testing capability regardless of solar position. The experimental system, show in Figure 19, was built on a mobile cart to allow for ease in solar alignment. The Fresnel lens measured 118 x 87 cm,1.06 m^2 in area, and had a focal length near one meter. A small mechanical oil pump was attached to a flexible vacuum hose and a 4-1/2 inch diameter chamber. The pyrolysis chamber was mounted on an extending, rotating arm, with height and angle adjustment to allow freedom of movement when adjusting, but fixed the chamber during tests to focus light directly on the sample. The mechanical pump was capable of achieving a system pressure of approximately 1 x 10^{-3} Torr. A scroll pump was added to the system to maintain a continuous gas flow from the pyrolysis chamber during vaporization to a storage system while achieving vacuum pressures. A scroll pump is critical in the operational system to transport the oxygen away from the pyrolysis system to the cryocooler while maintaining operational vacuum pressures. The scroll pump maintains a vacuum while moving camber gasses to a storage tank. Mechanical and oil pumps exhaust chamber gasses to the ambient environment.

Figure 19 – Fresnel Lens Vacuum Pyrolysis Experimental Setup

Multiple instruments were used to measure temperature, pressure, gas content, and solar flux. An analogue pressure gauge was attached to the system early in the testing phase to provide an estimate of chamber pressure. A convectron pressure transducer was added to the system to provide more accurate pressure measurements. The convectron had an operating range between atmospheric pressures down to 1 x10^{-3} Torr and read out to a digital display. Temperature measurement was done by a C-type thermocouple made of rhenium and tungsten placed directly

in the sample crucible during tests. The thermocouple had an operating range between 0 and 2300°C. A handheld pyrometer was used to measure sample temperatures in the case that the thermocouple failed during long duration tests.

To measure gas content, a residual gas analyzer/spectrometer was employed. The residual gas analyzer had much lower operating pressures than the main pumps were able to achieve. A precision leak value was used to leak gas from the higher pressure main system to the lower pressure gas analysis system. The gas analysis system preserved a high vacuum through the use of a turbo pump. An ion gauge was used to measure pressures between 10^{-3} and 10^{-12} Torr within the low pressure system. The residual gas analyzer communicated with a laptop computer, providing real time gas analysis during experiments.

The regolith simulant required a very high temperature crucible for pyrolysis. A zirconia (ZrO_2) ceramic crucible was selected to provide thermal stability at high temperatures, shown in Figure 20. Two zirconia crucibles were used. One of the zirconia crucibles was poorly manufactured and could not withstand the high thermal environment. High temperature metal crucibles were considered, but could become a safety hazard when placed in the pyrolysis environment. The crucible was approximately one inch in diameter and an inch in height. The crucible provided a small volume, less than forty grams of simulant, to be directly exposed to the focus of the Fresnel lens for vacuum pyrolysis.

Senior also suggested that electromagnetic stirring within the crucible is beneficial for good mass transfer, as only the top surface is exposed to concentrated radiation in pyrolysis[17]. Stirring best applies when the entire sample becomes molten. Higher temperatures than those in this experiment are required for stirring to be effectively employed.

Figure 20 - Zirconia Crucible Used

VI. Results

A total of eleven experimental tests were completed with the Fresnel lens pyrolysis system during this study. The temperature needed for partial vaporization and dissociation of the regolith simulants was achieved. The behavior and engineering challenges of oxygen production through vacuum pyrolysis were better understood from a series of eleven experiments involving ilmenite, enstatite, and MLS-1a regolith simulants. The limited area of solar capture and many power losses caused the Fresnel system to be unable to achieve necessary dissociation temperatures. The system shown above in Figure 19 was an iterative product of lessons learned through early tests. A full account of all experimental tests can be found in the Appendix B.

Initial testing aimed at familiarization of the Fresnel lens and pyrolysis system in winter solar conditions. The first test demonstrated the concentrating power of the Fresnel lens by it vaporizing zinc powder. The zinc vapors immediately condensed on the inner surface of the glass port, which partially blocked the solar radiation. The first test showed evidence of the greatest disadvantage of this system, that vapors would degrade the performance of the system by obstructing the path of the power source. The glass port cracked after the zinc condensate remained on the inner surface for approximately two minutes of operation, increasing the system pressure by an order of magnitude. Portions of the zinc powder sintered into crystals, but no melting or boiling was noticed. It was inferred that a very small amount of zinc achieved vaporization temperatures near 900 ^{o}C, but the thermal instrumentation was not used during this test.

Table 3 - Vacuum Pyrolysis Experiment Summary

Test	Date	Sample	Approximate Duration	Flux (W/m^2)	Initial Pressure (Torr)	Testing Pressure (Torr)	Max Temp (°C)	Mass loss
1	10-Jan	Zn	5m	-	$< 1x10^{-4}$	5	~900	-
2a	7-Mar	$FeTiO_3$	10 min	800	$< 1x10^{-4}$	$1.1x10^{-1}$	620	-
2b	7-Mar	$FeTiO_3$	15 min	945	$< 1x10^{-4}$	$2x10^{-2}$	>800	0.16%
3	18-Apr	$FeTiO_3$	~20 min	890	$6.0x10^{-1}$	$8x10^{-1}$	700	0.37%
4	3-May	$MgSiO_3$	<1min	955	$4.4x10^{-2}$	$4.4x10^{-2}$	548	0.05%
5	6-Jun	$MgSiO_3$	~30 min	940	$1.4x10^{-1}$	$2.3x10^{-1}$	1072	0.92%
6	16-Jun	Al_2O_3	20min w/ measurement One hour in total	950	$1.4x10^{-1}$	3	1800	-
7	17-Jun	$FeTiO_3$	1hour and 7 min	975	$2.3x10^{-1}$	1 - 4	1867	0.47%
8	12-Jul	$MgSiO_3$	~30 min	960	7	10	1100	10.66%
9	27-Jul	$FeTiO_3$	~30 min	795	$6.6x10^{-2}$	1.		0.73%
10	2-Aug	$FeTiO_3$	39 min	880	1.4	1 - 7	1436	0.37%
11	25-Aug	MLS-1a	52 min	1005	$9.6x10^{-2}$	$1.4x10^{-1}$	1474	10.1%

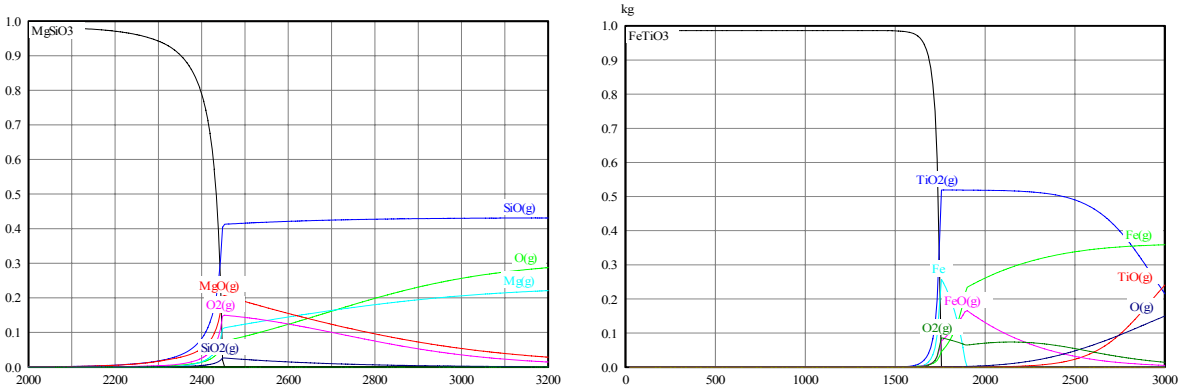

Figure 21 - Theoretical Dissociation of Enstatite and Ilmenite under experimental pressure (1 x 10^{-2} Torr)

To alleviate the vapor condensation problem on the inner surface of the glass port, the vacuum pump was left on during operations. It was hoped that the vacuum would establish a gas flow away from the glass port thus reducing the risk of accumulation and cracking. The C-type thermocouple and convectron pressure transducer were introduced to the system for the first ilmenite ($FeTiO_3$) test. A solar cell was also used to measure the ambient solar flux, accurate to the nearest W/m^2. The ilmenite samples were crushed to maximize surface area exposure. The theoretical dissociation of ilmenite at experimental conditions is show in Figure 21-B.

The convectron measured an initial increase in pressure of approximately one order of magnitude when solar radiation was focused on the 30 g sample of $FeTiO_3$. A maximum temperature of 620 ^oC was reached in the early test. It must be noted that the thermocouple was placed near the sample, and at times it was in direct contact with the ilmenite. The thermocouple was not always measuring the maximum temperature of the sample surface. It is best used as a reference temperature of the entire sample, not the sample surface. Poor quality crucibles were used initially, which severely cracked when thermally shocked. This test was halted once the crucible broke, thus affecting thermocouple measurements.

A later test was performed the same day with a larger solar flux, allowing much greater chamber temperatures. The afternoon test achieved temperatures greater than 800^oC, allowing a small portion of the ilmenite surface to boil. The test was again stopped when the crucible broke. Pressure increased during the application of radiation. Sample inspection showed melted portions of the ilmenite surface and a small mass loss.

A main concern for comparison between terrestrial experiments and oxygen production in the lunar environment is the trapped gasses that occur from natural atmospheric pressure on the Earth. In the first few experiments, it was not possible to conclude that the pressure increase is purely due to the vaporization of ilmenite or partially due to the out gassing of trapped gases within the rock. To determine the behavior of out gassing, both ilmenite ($FeTiO_3$) and enstatite ($MgSiO_3$) samples were placed in a vacuum and heated in an oven. The mass was measured at the beginning and end of each phase of the outgassing test. It was concluded that placing the rocks in a vacuum accounts for only a small percentage of offgassing mass loss, 0.06% for ilmenite and 0.035% for enstatite of the total sample. Heating the samples to approximately 700^oC had a much more profound affect than pulling a hard vacuum, but does not account for a

large mass loss. Approximately 0.65% of ilmenite mass and 0.69% of enstatite mass can be accounted for by releasing gases through heating. The offgassing results show that some of the experimental results exhibited melting but not significant vaporization, evidenced by similar mass losses to the offgassing cases.

Various methods to reduce window contamination and failure were attempted. The chamber was preheated to slowly raise the glass temperature and kovar seal so thermal shock would not occur when concentrated solar radiation passed through it. Windows composed of fused silica and sapphire crystal, capable of withstanding higher temperatures and larger thermal gradients, also failed to maintain a good vacuum. It was concluded that the problem was not associated with the thermal shock of the translucent material, but on the sealing material that bound the translucent to the vacuum chamber wall, and the coefficient of thermal expansion mismatch.

Summer conditions provided greater solar flux and better atmospheric transmission, providing much larger temperatures for pyrolysis. Figure 22-A shows that typical setup for applying concentrated solar flux through the vacuum chamber window. Tests five through eleven all reached maximum temperatures above one thousand degrees Celsius, and lost more mass than can be account for by offgassing. The aluminum oxide test was the first long duration exposure test completed. Despite continuing issues with windows cracking under thermal stress increasing the chamber pressure, it was of interest to see how the simulant would react to long duration exposure to concentrated solar flux. After a period of twenty minutes, the simulant became molten as shown in Figure 22-B. In the long duration tests, it was observed that the condensation of aluminum oxide vapors occurred cyclically. The area of solar flux passing through the glass flange would vaporize surrounding condensate while condensation would occur radially outward on the glass. The long duration exposure caused the thermocouple to completely disintegrate. Since no stirring was done, only the surface of the 20 gram sample was experiencing direct heating. Aluminum oxide below the surface was heated by conduction. It was observed that about one third of the sample by depth was completely melted together. Initially the sample was a fine talcum-like powder.

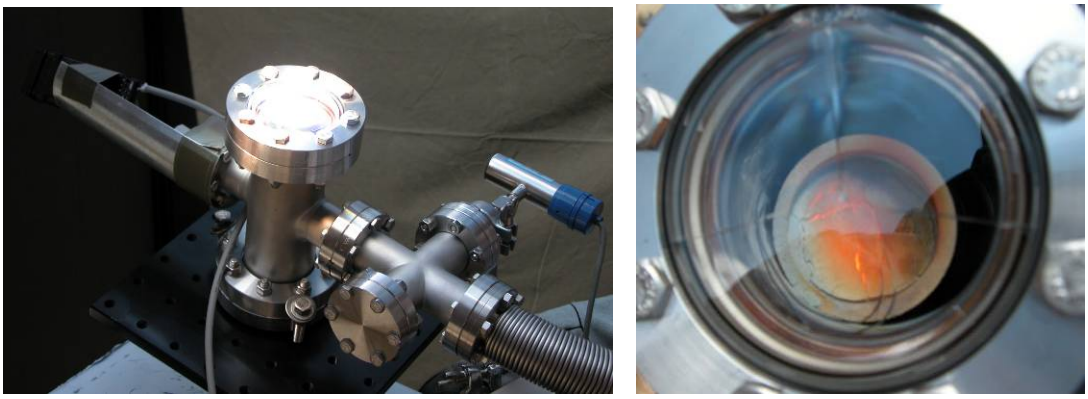

Figure 22 – (A) Chamber when focus is applied. (B) Molten aluminum oxide just after solar flux was removed

A long duration test was completed with ilmenite ($FeTiO_3$) in test seven. Initial sample boiling was observed within the third minute. Boiling continued sporadically throughout the one hour test depending on focal position, solar flux, and window contamination. Unfortunately, the thermocouple was again lost after 26 minutes of solar exposure. Its mass was not added to the

original sample mass, thus providing error in the final mass loss measurement. The small mass loss recorded is a sum of the mass gained from the introduction of the end of the thermocouple and the mass lost through vaporization. An ilmenite sample of thirty eight grams nearly melted completely. All rock fragments at least sintered together with the majority, more than three quarters, completely melted. As shown in Figure 23-A, the focus was placed on the left side of the sample while the right side of the sample was heated by conduction only. Liquid ilmenite and reduced oxide slag was spattered against the crucibles walls while ilmenite vapor both condensed on the window, crucible, and chamber. The experiment was forced to terminate when the temperature of the glass became too hot to sustain structural integrity. Figure 23-B shows the depression formed when the structurally unsound glass flange was still attempting to hold a rough vacuum.

Figure 23 – (A) Melted Ilmenite with spatter and condensation on crucible walls. (B) Melted glass flange

A scanning electron microscope was used to do a spectral analysis of the sample after testing. It measured a decrease in the proportion of oxygen with an increase in the proportion of metals on the sample surface when compared with the sample before testing. This is evidence of some dissociation and condensation to free a small potion of gaseous oxygen.

Enstatite was tested in the eighth test under similar conditions as test seven. There was a significant problem with condensation forming on the glass flange, shown in Figure 24. It was concluded that enstatite forms condensate much more readily than ilmenite under similar conditions. The condensation caused a reduction of chamber temperature; however, a maximum temperature of 1300 ^{o}C was maintained throughout the test. Thirty minutes of solar exposure yielded a mass loss of ten percent. Approximately one gram of enstatite was completely vaporized, condensing away from the crucible.

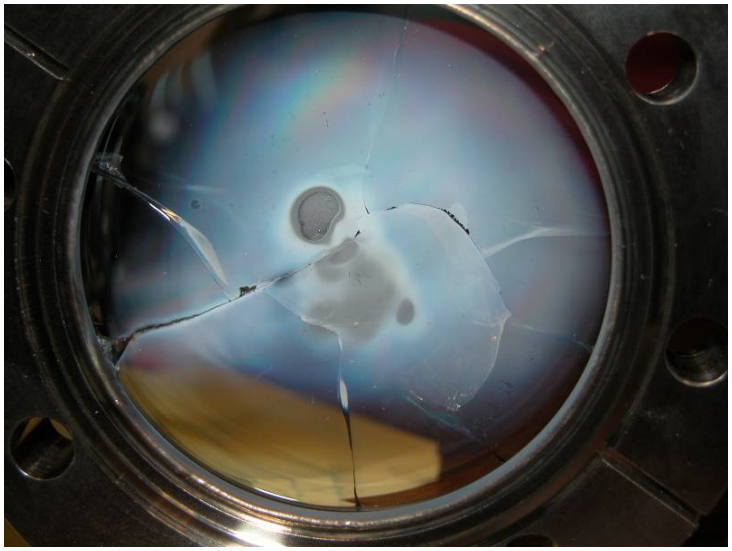

Figure 24 – Simulant condensation on glass vacuum seal flange

The ninth test employed the residual gas analyzer for direct oxygen detection and other residual gas analysis. The RGA required low pressures for operation, so a separate turbo vacuum system was built connecting to the pyrolysis flow by a leak value. The gasses resulting from pyrolysis and condensation were leaked into the high vacuum system for analysis. Although the conditions during the test did not provide many periods of high intensity sunlight, the RGA did measure an increase in relative partial pressure of oxygen in the gas flow shown below in Figure 25. The RGA measures concentrations of hydrogen, water vapor, nitrogen, carbon dioxide and water on a logarithmic scale. The partial pressure of oxygen gas increased significantly when a high solar flux was focused on the sample at minute marker 19.5. The amount of oxygen gas rose much more than any of the other gasses, thus providing rational for the argument that some oxygen gas did dissociate from the sample and remained in the gas flow after the suboxide or metal species condensed.

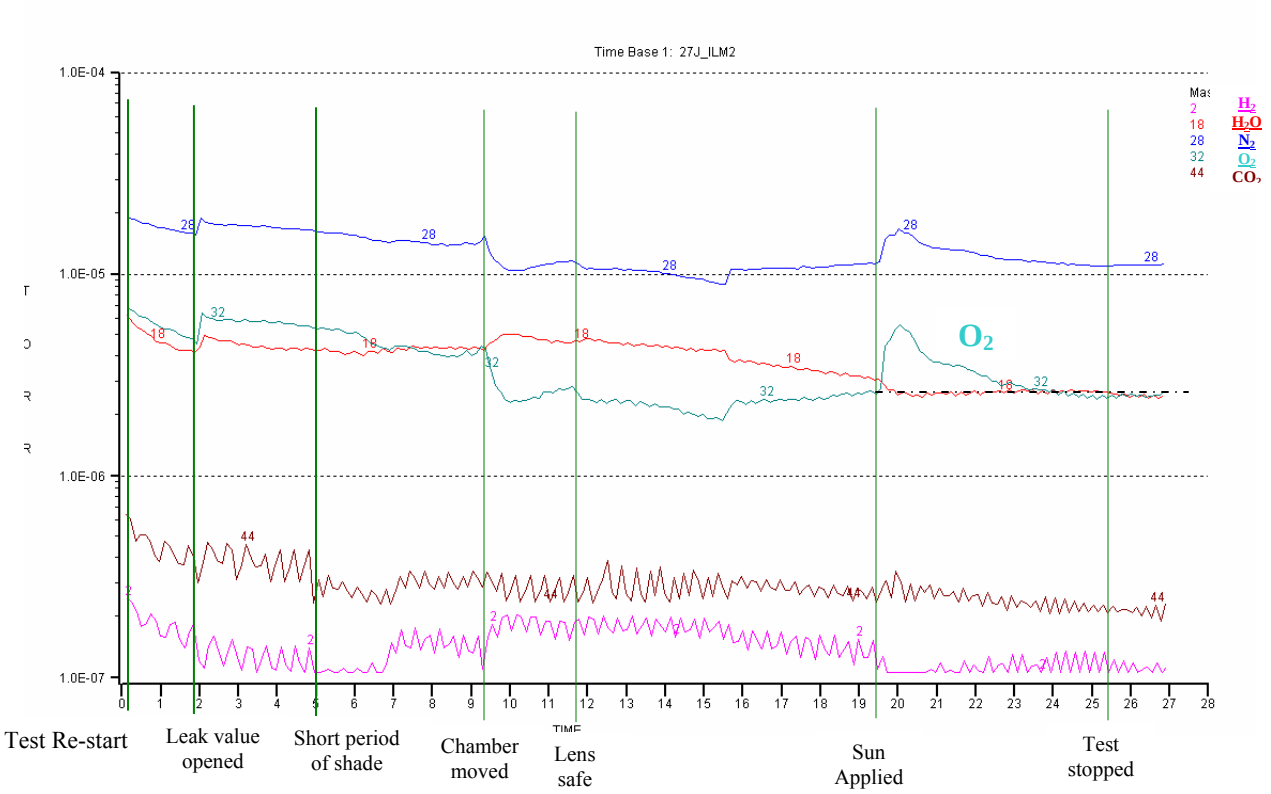

Figure 25 – Ilmenite test with cracked window (partial pressure vs. time)

Since the conditions did not provide the best solar flux in the previous test, experiment ten was a continuation of experiment nine in more favorable conditions. In addition, a fan blowing air and boiloff from a liquid nitrogen dewar were used to cool the temperature of the glass so that it would not crack. The boiling nitrogen was guided by a length of refrigerant tubing on released directly on to the outside surface of the glass flange to minimize the formation of a strong thermal gradient. The cool nitrogen gas would remove energy from the glass and chamber while the fan convected heat away to the surrounding thermal reservoir. An infrared thermometer was used to measure the surface temperature of both the glass and the steel chamber wall. To reduce thermal shock, the chamber was slowly exposed to the full focus of the Fresnel lens over a period of about four minutes. The temperature of the chamber at the focus was approximately 500^{o}C once it was fully exposed. At the same time the glass temperature was approximately 100^{o}C. The glass flange lasted for a total of twelve minutes during operation, breaking at 200^{o}C; however, the temperature of the glass where condensation was present was higher, near 300 ^{o}C. It was concluded that there exist thermal stresses despite cooling efforts within the system that require different materials for operations to be successful. The sample did melt and boil during periods of solar exposure, but the boiling was restricted due to heavy condensation on the glass. The mass lost was very small and inconclusive of oxygen separation.

The University of Minnesota provided a small sample of its MLS-1a lunar regolith simulant. This simulant was designed to chemically represent the Apollo 11 mare regolith found in the Sea of Tranquility. Although it does not have a similar physical makeup of agglutinates, the chemical similarities between MLS-1a and lunar regolith provide good comparisons when trying to understand behavior of oxide dissociation and oxygen liberation. In addition, the MLS-1 was

a fine talcum like powder. The ilmenite and enstatite samples were crushed rock. A trend that was noticed early on in testing was that increasing the surface area of the sample increased the ability of the simulant to vaporize.

Results from tests conducted with a CO_2 laser to determine condensing characteristics of oxides concluded that the condensing surface must be relatively close to the vaporous oxides.[9] It must also be hot enough to reduce the oxygen sticking coefficient, but be cool enough to condense only suboxides and metal vapors to allow oxygen gas to escape. C.L. Senior estimated that more oxygen would be produced with a 700 ^{o}C than a 20 ^{o}C condensing surface.[22] Instead of placing an object into the chamber, the chamber walls were used as the thermal gradient surface. In test 11, a cooling loop was built to conduct heat away from the steel so that condensation would increase. It consisted of flexible copper tubing to pass water through 15 loops wrapped tightly around the chamber. Also, a secondary transparent barrier was placed directly over the top of the crucible to deflect vapors away from the main glass flange, and favorably condense on the secondary barrier than the main glass.

Very good solar fluxes allowed for a high temperature test. The buried thermocouple measured 1320^{o}C in the local area of heated simulant at its maximum during the test. Pressure initially rose by 0.044 Torr when the simulant was exposed to focused sunlight. The glass flange broke in the fifth minute of operation, but a rough vacuum was maintained for the remainder of the test. Unfortunately the RGA overpressurized, and thus was unable to measure partial pressures of gaseous species. Since the solar conditions were so good, the regolith simulant was heated for another forty minutes. During this time, boiling was continuous, but occurred at various strengths and locations depending on the tightness of the focus. When the test was complete, the simulant was observed to be completely melted and partially vaporized, as shown below in Figure 26. The thermocouple had become fused into the sample. Mass loss was recorded as ten percent, but error was present from portions of broken crucible and the thermocouple leads that became fused. The error margin is arguably 2 – 3%. This final test provides evidence of oxide vaporization when exposed to high temperatures for long duration.

Figure 26 - MLS-1a simulant completely melted and partially vaporized after testing

VII. Case Study Comparison

In 2004, President George W. Bush introduced the Vision for Space Exploration that included a new architecture to replace the Space Shuttle for manned spaceflight. NASA commissioned the Exploration Systems Architecture Study (ESAS) to provide general design requirements for the next generation human rated vehicle. The study recommended a vehicle similar to Apollo, called the Crew Exploration Vehicle shown in Figure 27. The CEV is a modular, capsule-based approach that plans to be the foundation for a sustainable human and robotic space exploration program. It is larger in volume that the Apollo capsule but only slightly heavier. The CEV provides much greater flexibility to serve various exploration possibilities to the Moon. The proposed propulsion system for the CEV is designed to take advantage of *in situ* propellant production, specifically lunar oxygen production and Martian methane production. "A lunar outpost just 3 days away from Earth will give us needed practice of 'living off the land' away from our home planet, before making the longer trek to Mars."[23] The engines for the service module and lunar ascent stage are a methane-oxygen mixture, providing NASA numerous hours of operational methane engine experience before employing one for Mars missions. The service module provides lunar orbit insertion burns on the way to the Moon and transearth injection burns when returning home.

Disadvantages of using pure liquid oxygen as an oxidizer are safety and storability. Liquid oxygen will boil off when raised above –183 ^{o}C, requiring insulation for storage tanks. Cryogenic propellant formulations are commonly restricted to boost engines which can vent fuel tanks continually while on earth, topping off minutes before ignition. Cryogenic oxygen is also a large safety hazard. Storing LOX onboard a spacecraft increases the risk of fire. Hypergolic propellant formulations have better storability characteristics, but are toxic and very difficult to handle.

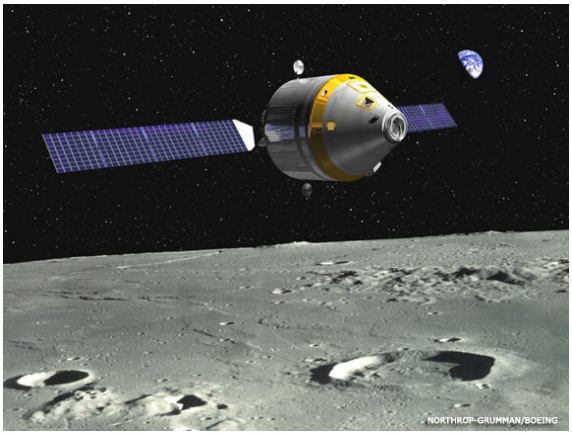

Figure 27 - The Crew Exploration Vehicle Concept

The second propellant combination is a hydrogen-oxygen mixture, used in the lunar descent engine. Hydrogen-oxygen engines are the most efficient engines available. Although typically used for orbit insertion, this architecture aims to use LH_2-LOX for a variety of maneuvers. The architecture allows for the possibility to fly to the Moon without a full compliment of ascent stage propellant. The crew of that mission would produce oxygen on the surface of the Moon

and store it in available empty tanks. The crew would then have the necessary propellant ascent to the orbiting service module, and surface maneuvers. In the CEV rollout presentation, NASA Administrator Griffin remarked "The architecture can make significant use of lunar resources. At first, in all likelihood oxygen obtained by [solar] roasting [of regolith], if the availability of either water ice or hydrogen in other forms at the lunar poles is ultimately confirmed, then we will be able to extract hydrogen from the moon and would have the constituents of the most important propellant combination for at least the next several decades right there on the moon."[3]

There are a variant of mission concepts that are capable of reaching the Moon for exploration, habitat servicing, or transportation. The two most common mission plans for lunar operations are direct ascent and lunar orbit rendezvous. A direct ascent mission plan transports the entire spacecraft architecture to the lunar surface, while a rendezvous approach only takes the necessary hardware for lunar surface operations while the remaining transport architecture stays in lunar orbit. The Apollo program employed the lunar orbit rendezvous mission strategy using the Lunar Module (LM) for surface operations while the Command and Service Modules (CSM) remained in lunar orbit. Either mission plans can improve by the implementation of a lunar oxygen production facility. In the interest of improving fuel efficiency, it is likely that future lunar missions will adopt a strategy of in situ oxygen production with lunar orbit rendezvous.

The Apollo program is used as a case study for mass savings possible assuming all the oxidizer would be supplied by the lunar production plant. These include the ascent stage of the LM, and the service module engine. The service module engine is used to transport the CSM from lunar orbit to earth rendezvous. All propellants for the ascent propulsions system and service propulsions system are nitrogen tetroxide and a fifty-fifty blend of unsymmetrical dimethyl hydrazine and hydrazine. The hypergolic combination of hydrazine (N_2H_4) and nitrogen tetroxide (N_2O_4) have flight proven reliability in the US Space program for orbital maneuvering, transplanetary injection, and attitude control. The only hypergolic combination with liquid oxygen is Analine ($C_6H_5NH_2$), which is unlikely to be used as a future lunar mission propellant.

There are two main phases where an *in situ* oxidizer would replace terrestrial propellant: The ascent from the lunar surface and return from the Moon to the Earth, which includes orbit injection and correctional burns. An operational history of the ascent stage of the Apollo Lunar Module is summarized below in Table 4. All Apollo missions were constrained to operations near the lunar equator. The ascent propulsion system required approximately 3000 lbs of oxidizer to provide enough propulsive power to launch the ascent stage off the lunar surface and rendezvous with the orbiting CSM. Increasing the capability of the CEV to serve all lunar locations would increase the requirement for propellant above 3000 lbs, but this example serves as a benchmark for savings that *in situ* propellant production can provide.

LM Ascent Stage Propellant Status						
Total Consumed (lbs)	Apollo 11	Apollo 12	Apollo 14	Apollo 15	Apollo 16	Apollo 17
Fuel	1856	1862	1879	1893	1870	1918
Oxidizer	2980	3005	3014	3052	3011	3059
Total	4836	4867	4893	4945	4881	4977

Table 4 - Propellant Proportion Burned in Apollo Mission Lunar Ascents[24]

The ascent stage could reduce approximately 61% of its fuel weight if the oxidizer portion of the ascent propellant combination were produced with vacuum pyrolysis or another form of *in situ* oxygen production. This translates into savings associated with all propulsive burns occurring before surface operations. All of the propellant that was produced on the moon would normally have been transported from the earth to the moon. The velocity changes, ΔVs, necessary for spaceflight are dependent on the orbital dynamics and are similar for spacecraft variants, assuming negligible gravity losses. Assuming a constant nozzle exit velocity for a chemical rocket combination, propellant requirements are driven by inert mass. Oxidizer and fuel that is not being used in the respective burn is inert mass, increasing the required propellant for achieving a velocity change. The relationship between velocity change, nozzle exit velocity, and mass change is known as the ideal rocket equation[25].

$$\Delta V = -V_{exit} \ln\left(\frac{m_{final}}{m_{initial}}\right)$$

The second phase where *in situ* propellant production can offer savings is for the service module propulsions system. This system provides propulsion for transearth injection and midcourse corrections when flying from the Moon to the Earth. Table 5 summarizes Apollo mission weights before and after transearth injection. It took approximately 6000 lbs of oxidizer to change the CSM's orbit to rendezvous with Earth.

Mission Weights following Lunar Surface Departure (lbs)						
	Apollo 11	Apollo 12	Apollo 14	Apollo 15	Apollo 16	Apollo 17
CSM at Docking	36847	35306	34125	35928	38452	36036
CSM at Pre-entry Separation	26656	25444	24375	26323	27225	26659
Propellant Used	10191	9862	9750	9605	11227	9377
Oxidizer Consumed	6278	6075	6006	5917	6916	5776

Table 5 - Propellant Consumed During Missions Phases of the SM Engine[24]

Assuming the oxidizer for both the lunar ascent and transearth injection burns is completely supplied by a production plant on the Moon, the mass savings for the entire flight can be calculated. Propellant mass will be saved on launch, translunar injection, midcourse correction, and lunar orbit insertion burns by reducing the initial launch mass. The Apollo 11 case is used as an example. In this flight, approximately 9258 lbs of oxidizer was used during lunar ascent and transearth injection that could be produced on the Moon. The NASA history office provided propellant consumption figures at each stage of the flight. Knowing the inert mass for each stage, the total initial and final weights are found corresponding to each burn. The mass produced through *in situ* resource utilization is simply subtracted from the initial mass. Assuming the nozzle exit velocity remains constant, the final mass is solved using the ideal rocket equation. Table 6 summarizes the propellant mass savings for the Apollo 11 case. Over 55,000 lbs of total mission propellant can be saved at launch by producing 9,200 lbs of oxidizer on the Moon. The benefits can be seen as either a 9200 lb extra payload capacity or a reduction in the size of the launch vehicle.

Apollo 11 - Burn Description	Δ V (ft/s)	Initial Mass (lbs)	Final Mass (lbs)
Translunar Injection			
S-IC Burn	7728	6477875	1817735
S-II Burn	13591	1444200	481388
S-IVB 1st Burn	2868	367834	298609
S-IVB 2nd Burn	10008	261935	100756
Lunar Orbit Insertion	3082	96261	72336
Modified Translunar Injection			
S-IC Burn	7728	6468617	1815137
S-II Burn	13591	1434942	478302
S-IVB 1st Burn	2868	358576	291093
S-IVB 2nd Burn	10008	252677	97195
Modified Lunar Orbit Insertion	3082	87003	65379
In Situ Produced Oxidizer	**9258**	**lbs**	
Total Launch Mass Savings	**55548**	**lbs**	

Table 6 - Apollo 11 Burn Data and Propellant Mass Savings from ISRU[24,26]

The Crew Exploration Vehicle will have similar propellant savings when oxidizer is produced through *in situ* resource utilization. Differences in the CEV including mass, propellant mixture, engine design, flight dynamics, and the launch configuration will alter the benefits of producing oxidizer on the Moon. However, it is clear that producing oxygen on the lunar surface translates into considerable propellant and cost savings.

VIII. Demonstration Mission

All of the available technologies for the *in situ* production of oxygen require further development to achieve a practical system. The current level of technology readiness of vacuum pyrolysis is at TRL 3, where experiments have provided characteristic proof of concept. Improving the state of technology readiness through subsystem, environmental and operational tests will lead to a demonstration of *in situ* resource utilization on the Moon.

As the technology for vacuum pyrolysis improves, its enabling architecture must meet programmatic, environmental, performance, and operational requirements. The cost of building and transporting the hardware necessary for oxygen production on the lunar surface shall offset the costs of launching the full mission complement of oxygen from Earth. This may be unlikely initially as there will be few lunar flights per year that are capable of using *in situ* oxygen. The lessons learned from the initial phase of operations are expected to apply to the exploration of other bodies and planets. The technique shall allow for scalable development. Initially, vacuum pyrolysis systems will be very small, increasing as it becomes better understood in an operational environment. The production plant will be sized according to expected demand and efficiency. The system must exhibit high reliability and require minimal maintenance.

Significant environmental challenges present on the lunar surface must be overcome for resource utilization. The equipment used must withstand thermal shifts between lunar day, approximately 400 K, and lunar night, approximately 100 K. Reaction forces that terrestrial mining equipment use for operations are different on the lunar surface due to smaller gravitational forces ($g = 1.6$ m/s^2). This will force new engineering designs for seemingly simple tasks of digging, lifting, and hauling material. Machines require materials that are built for operations in vacuum (10^{-9} to 10^{-12} Torr). Since lunar soil is very fine, dust accumulation could wreck havoc on seals, friction bearings and other moving parts. A lunar day cycle of 336 continuous hours supplies a high solar flux (~1388 W/m^2), with intense radiation, flares, and the solar wind. The equipment must also be shielded from micrometeorite impacts, and withstand dust contamination.

The resource utilization system must meet a variety of performance requirements. Vacuum pyrolysis production plants shall meet production rate metrics depending on the mission architecture it will augment. Pilot plant production metrics range from two to ten metric tons of oxygen per month to support a four astronaut crew sized mission. Theoretically vacuum pyrolysis is capable of achieving nearly 0.13 kg O_2 produce for 1 kg of regolith supplied. The production metrics required also depend on the propellant combination used. A hydrogen-oxygen system has an operational oxidizer to fuel ratio of 6:1 while methane-oxygen has a lower oxidizer ratio of 4:1. The plan design may be built as a single unit or on a modular basis. Each method carries a unique advantage. A single plant requires only one launch, immediately allowing for oxygen production to begin. A modular system may require more than one launch, take longer to set up, but allows for a more adaptable system. When the demand for oxygen is increased, more modules may be brought online for a larger production rate. The power requirements for vacuum pyrolysis are very high due to the high chamber temperatures necessary for molecular dissociation. Eagle Engineering estimates that a pilot plant will require an estimated 35.5 MW-hr/mt O2 produced; however, 25.5 MW-hr/mt O2 of that total is for regolith

vaporization, which comes from direct solar flux. Lunar production facilities shall minimize the need for re-supply. An ideal production plant will operate autonomously using only resources available on the Moon once operations have begun. No re-supply is needed from Earth for the vacuum pyrolysis technique. Surface excavation of regolith is the primary supply for oxygen production plants. This can be accomplished by a rover that can both dig and haul regolith from the excavation site to the pilot plant, similar to load-haul-dump machines used in US mines.

The application of vacuum pyrolysis into an augmenting infrastructure will be an evolutionary process. Various developmental milestones have been identified in Figure 28 that improve the technique to an operational level. Three flights are critical to this evolution. The *instrument/volatiles* mission will demonstrate the ability to roast lunar regolith to collect volatile elements (H, He, C, N). It will provide an evaluation of solar concentration in the lunar environment, the materials used, and the instrumentation measuring and controlling the system. This mission advances the technology to TRL 5. The second flight, *the demonstration mission*, requires further development of those components which were not direct heritage from the instrument flight. This mission improves upon the volatiles flight in that it is fully capable of producing oxygen from lunar regolith. Higher temperatures are gained from a more powerful concentrator. This will also be the first environment test of the condenser system. The *pilot plant* mission will fully employ the vacuum pyrolysis technique to produce oxygen to augment the mission. The pilot plant serves as a prototype for a future production plant. Oxygen production efficiency will be investigated and exploited, as well as incremental improvements made as the technology evolves. The lessons learned from the oxygen pilot plant will be applied to all other forms of ISRU as exploration continues to other celestial bodies.

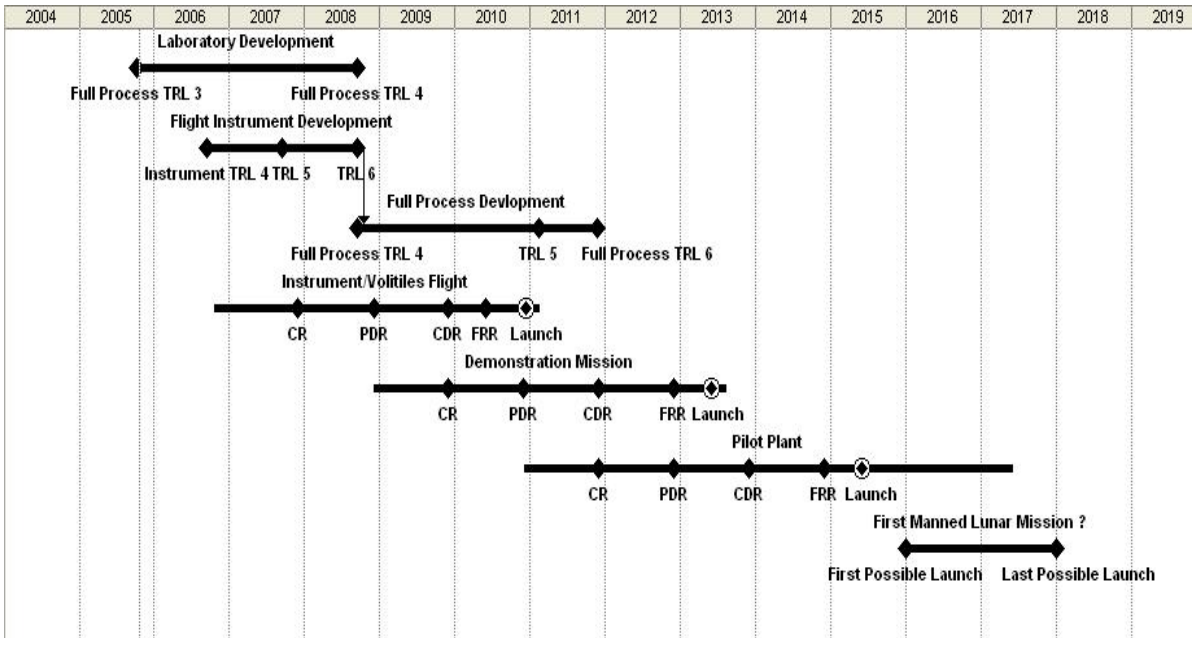

Figure 28 - In Situ Resource Utilization for the Production of Oxygen Mission Plan[27]

IX. Conclusions

The experiments completed in this investigation build on previous research to demonstrate the feasibility of the vacuum pyrolysis technique for the production of oxygen in the lunar environment. Experiments were conclusive that focused solar energy can vaporize and dissociate terrestrial lunar regolith simulants. Samples of approximately 20 grams were fully melted and partially vaporized. Measurements in mass loss and scanning electron microscopy reveal a decrease in oxygen after the application of solar energy. Maximum mass loss due to vaporization was approximately 10 % of the sample. Maximum chamber temperature reached was approximately 1900^{o}C while most experiments operated between 900 - 1400 ^{o}C.

Further research is needed in condensation and distillation behavior of oxides to advance the level of technology readiness of the vacuum pyrolysis process. A new window diesign is needed to survive a high rate of thermal change and long exposures to solar radiation. A window with minimal transmission losses is ideal for this application due to the exposures of up to 300 hours on the Moon. A larger Fresnel lens or other concentrating device is needed to provide more power to regolith simulants. Boiling only occurred at very high temperatures, at times difficult to maintain. A more powerful system would provide for a greater portion of the oxides to dissociate. A challenge in this experimental setup was the operation of two vacuum chamber connected by a precision leak valve. According to equilibrium calculations, the temperature required for dissociation decreases logarithmically as pressure decreases. An experimental system at low pressure (1×10^{-6} - 1×10^{-9} Torr) is also more favorable for precise mass spectrometry. Maintaining a high vacuum would allow a residual gas analyzer to measure real time oxygen partial pressures in the gas stream without over pressurization. A full understanding of regolith dissociation will be necessary to increase the efficiency of the system. The reduction behavior of pyroxene, feldspar, olivine ilmenite and spinel will constitute the majority of oxygen produced.

Estimates of the costs of transporting materials from the earth to the Moon range from $20,000 to $30,000 pound.[28] Human settlement of space must eventually involve the utilization of space resources. Oxygen production is just one form of in situ resource utilization. Simplicity, low energy, easily attainable feedstock, and resupply mass are the keywords for the processes that will ultimately be selected for the initial production of oxygen on the moon. The most likely candidates for oxygen production on the moon are vapor pyrolysis; glass reduction with H_2; molten silicate electrolysis; ilmenite reduction with H_2, CO, and CH_4; fluxed molten silicate electrolysis; and ion plasma pyrolysis. However, it is too early in the development of all of these processes to eliminate any from consideration.[28] The reduction of ilmenite by hydrogen gas has been given the greatest amount of study with the best results to date. The other six techniques have seen very little experimental results. The reduction of ilmenite by hydrogen gas provides an oxygen yield of 0.104 g O_2 produced at 1000^{o}C for every gram of ilmenite collected. The vacuum pyrolysis technique has a theoretical O_2 yield is 0.140 g O_2 produced for every gram for mare regolith at 10^{-6} Torr at 1400 ^{o}C. The system mass of a pyrolysis plant is estimated to be half the size of a comparable reduction by hydrogen reduction plant using only ten percent of the power. The advantages that vacuum pyrolysis has over the reduction of ilmenite is that any form of regolith can be used, the process is very simple, and the process is well understood. The

ilmenite reduction technique must filter regolith for rich ilmenite ore, and provide the resupply of hydrogen gas.

The savings for a lunar mission have been demonstrated using the Apollo missions as a case study. Ideas for how in situ resource utilization for the production of oxygen in the Crew Exploration Vehicle have been introduced. Finally requirements were written for an oxygen production plant operating on the Moon. Milestones were established to provide an evolutionary plant to a successful oxygen pilot plant.

X. References

1. Schrunk, Burton, Bonnie and M Thangavelu. The Moon: Resources, Future Development and Colinization. John Wiley and Sons. New York, 1999

2. Sanders, Gerald. "In-Situ Resource Utilization (ISRU) Capabilities & Roadmapping Activities". LEAG/SSR Meeting October 2005. NASA JSC

3. Griffin, Mike. NASA Headquarters News Conference to release the Exploration System Architecture Study results. September 19, 2005

4. Cardiff, Eric, Pomeroy, Brian and John Matchett. "The Vacuum Pyrolysis Technique of In Situ Oxygen Production." LEAG/SSR Meeting October 2005. NASA GSFC

5. Mankins, John. *Technology Readiness Levels: A White Paper*. Advanced Concepts Office, NASA 1995

6. Lewis, J., Matthews, M., and M. Guerrieri. Resources of Near-Earth Space. The University of Arizona Press. Tuscon, 1993

7. Steurer, Wolfgang. *Vapor Phase Pyrolysis*. In Space Manufacturing. 1985

8. Senior, Constance L. "Solar Heating of Common Lunar Minerals for the Production of Oxygen". PSI Technology Corporation. Journal of the British Interplanetary Society, 44, 579-588, 1991

9. Pomeroy, Brian. *Vacuum Pyrolysis Under Graduate Thesis*. To Be Published. Penn State University, 2006

10. Stump, Chistiansen, Euker. *Conceptual Design of a Lunar Oxygen Pilot Plant*. Eagle Engineering. NASA Contract Report NAS9-17878. July, 1988

11. Taylor, Larry. *Physical and Chemical Characterization of Lunar Regolith*. Planetary Geosciences Institute – The University of Tennessee (Jan 2005).

12. Heiken, G, Vanimand D and Bevan French. The Lunar Sourcebook: A User's Guide to the Moon. Cambridge University Press 1991 New York

13. Jordan, J.L. *Lunar Hydrogen and Other Volatiles*. Lamar University. AIAA 92-1665. AIAA Space Programs and Technologies Conference. Huntsville, Al 1992

14. ASTM. *Standard – Solar Constant and Zero Air Mass Solar Spectral Irradiance Tables*. West Conshohocken, PA

15. ASTM. Standard *Tables for References Solar Spectral Irradiance at Air Mass 1.5: Direct Normal and Hemispherical for a 37^{o} Tilted Surface*. West Conshohocken, PA

16. MDC Vacuum Products. Viewport, zero profile 7056 Glass http://www.mdcvacuum.com

17. Senior, Constance L. "Lunar Oxygen Production by Pyrolysis". PSI Technology Corporation. Resources in Near Earth Space The University of Arizona Press. Tuscon, 1993

18. Brewer, Leo. *The Thermodynamic Properties of the Oxides and Their Vaporization Processes*. University of California. Berkley, 1952.

19. Lide, David. CRC Standard Thermodynamic Properties of Chemical Substances. The Handbook of Chemistry and Physics. 85th Edition. CRC Press 2005

20. Roine, Antti. Outokumpu HSC Chemistry for Windows – Chemical Reaction and Equilibrium Software with Extensive Thermochemical Database. Version 5.11. Outokumpu Research Oy, Finland 2002.

21. Kulikov, I.S. Thermal Dissociation of Chemical Compounds. Translated from Russian by J Schmorak. Moscow, 1966

22. Senior, Constance L. "Lunar Oxygen Production by Pyrolysis of Regolith". PSI Technology Corporation. 92-1663, AIAA Space Programs and Technologies Conference, March 24-27. AIAA, 1992, Huntsville, AL.

23. National Aeronautics and Space Administration. *How We'll Get Back to the Moon*. Crew Exploration Vehicle Introduction. www.nasa.gov/exploration

24. Orloff, Richard W. *Apollo by the Numbers: A Statistical Reference*. NASA History Division Office of Policy and Plans. NASA Headquarters. 2000 http://history.nasa.gov/SP-4029/SP-4029.htm

25. Humble, R, Henry, G, and Larson, W. Space Propulsion Analysis and Design. Space Technology Series. McGraw-Hill NY, 1996

26. NASA. *Apollo 11 Final Flight Plan*. Manned Spacecraft Center. Houston, TX. July 1, 1969

27. Matchett, J, Pomeroy, B, and Cardiff, E. *An Oxygen Production Plant in the Lunar Environment: A Vacuum Pyrolysis Approach*. Space Resources Roundtable VII (2005). League City, TX

28. Taylor, L and D Carrier. Pro*duction of Oxygen On the Moon: Which Processes are Best and Why*. AIAA Journal Vol 30, No 12, December 1992

Acknowledgements

The author would like to thank Dr. Eric Cardiff and Brian Pomeroy at NASA Goddard Space Flight Center for their assistance in the lunar oxygen project. Brian Pomeroy at NASA GSFC was responsible for the completion of the outgassing tests. Dr. Eric Cardiff was responsible for all scanning electron microscopy measurements.

Appendix A

Thermodynamic Data

CRC Standard Thermodynamic Properties of Chemical Substances

	Crystal Solid				Gas			
	ΔH_f KJ/mol	ΔG_f KJ/mol	S J/mol-K	C_P J/mol-K	ΔH_f KJ/mol	ΔG_f KJ/mol	S J/mol-K	C_P J/mol-K
O					249.2	231.7	161.1	21.9
O_2					0		205.2	29.4
O_3					142.7	163.2	238.9	39.2
Al_2O_3	-1675.7	-1582.3	50.9	79				
Al_2O					-130	-159	259.4	45.7
AlO					91.2	65.3	218.4	30.9
Al	0		28.3	24.4	330	289.4	164.6	21.4
CaO	-634.9	-603.3	38.1	42				
Ca	0		41.6	25.9	177.8	144	154.9	20.8
CrO								
CrO_2	-598							
CrO_3					-292.9		266.2	56
Cr_2O_3	-1139.7	-1058.1	81.2	118.7				
Cr_3O_4	-1531							
Cr	0		23.8		396.6	351.8	174.5	20.8
FeO	-272							
Fe_2O_3	-824.2	-742.2	87.4	103.9				
Fe_3O_4	-1118.4	-1015.4	146.4	143.4				
Fe	0		27.3	25.1	416.3	370.7	180.5	25.7
K_2O	-361.5							
KO_2	-284.9	-239.4	116.7	77.5				
K_2O_2	-494.1	-425.1	102.1					
K	0		64.7	29.6	89	60.5	160.3	20.8
MgO	-601.6	-569.3	27	37.2				

Mg	0		32.7	24.9	147.1	112.5	148.6	20.8
MnO_2	-520	-465.1	53.1	54.1				
MnO	-385.2	-362.9	59.7	45.4				
Mn	0		32	26.3	280.7	238.5	173.7	20.8
Na_2O	-414.2	-375.5	75.1	69.1				
NaO_2	-260.2	-218.4	115.9	72.1				
Na_2O_2	-510.9	-447.7	95	89.2				
Na_2					142.1	103.9	230.2	37.6
Na	0		51.3	28.2	107.5	77	153.7	20.8
P_2O_3								
P_4O_6								
P_2O					-279.9	-281.6	252.1	39.5
PO					-28.5	-51.9	222.8	31.8
P	0		41.1	23.8	316.5	280.1	163.2	20.8
SiO								
SiO_2								
Si	0		18.8	20	450	405.5	168	22.3
TiO	-519.7	-495	50	40				
TiO_2	-944	-888.8	50.6	55				
Ti_2O_3	-1520.9	-1434.2	78.8	97.4				
Ti_3O_5	-2459.4	-2317.4	129.3	154.8				
Ti	0		30.7	25	473	428.4	180.3	24.4
		30.7						

Blank Cells do not have any values

ΔH_f Standard Molar Enthalpy (heat) of formation at 298.15 K in KJ/mol

ΔG_f Standard Molar Gibbs energy of formation at 298.15 K in KJ/mol

S Standard Molar Entropy at 298.15 K in J/mol K

C_P Molar Heat Capacity at constant Pressure at 298.15 K in J/mol K

Appendix B

Test Reports

10 Jan 2005
Test 1
Initial Chamber Test

Observations

Today's test was the first complete solar test to include the vacuum system integrated with the Fresnel lens. Approximately 2-3 grams of zinc powder was placed into a zirconium crucible surrounded by another zirconium crucible resting on a zirconium perch.

The test was conducted in the afternoon at approximately 2:00 pm EST. The cloud cover reduced the solar flux significantly, which in turn lowered maximum available temperatures at the focus. Ambient temperature was near 55 degrees Fahrenheit.

Dr. Eric Cardiff and John Matchett adjusted the chamber angle parallel with the sun and lens. The chamber was elevated so that the focus of the fresnel lens was located in the crucible heating the zinc. Once the setup was adjusted properly the system was pumped down to vacuum. The initiation of vacuum altered the position of the zinc away from the focus. The chamber and system initially were at vacuum (~ 0 Torr).

The zinc was rapidly heated for approximately 5 minutes. Within the first 3 minutes the zinc was observed to be condensing on the glass surface. The condensed zinc would then vaporize again, and then condensed in a nearby region away from the focus. The glass window cracked in three places due to superheating. The system pressure steadily increased after rupture. The pressure before rupture was roughly 5 Torr. For safety reasons the experiment was terminated immediately and the area cleared.

Discussion

Evidence of the zinc powder condensing on the surface of the glass suggests that the zinc surpassed its vaporization temperature of 1180 K. Only a very small portion of the zinc in the crucible reached temperatures this high. There was evidence of zinc crystals, one large crystal and many small crystals precipitating from the powder. The crystals are shown below in figure 1. Most crystals were formed where the zinc was in contact with the crucible. Crystals indicate that the zinc powder was heated to a molten state (melting temperature of 693 K) and then cooled once the glass cracked and the experiment terminated. Since the majority of the zinc remained in powder form, the crucible's mean temperature did not exceed 693 K.

Figure 29 - Zinc Crystals after Solar Heating

Recommendations

If the system remained in operation for a much greater length of time, the entire 2-3 grams of zinc may have reached a molten state inside the crucible.

Superheating broke the chamber glass. To alleviate this stress, the vacuum pump will continue operation during all tests.

7 March 2005
Test 2
First test at 1100 hours, second test at 1400 hours

Initial Ilmenite Test

Observations
First Test:
Initial Flux: 790 – 805 W/m^2
Initial temperature: 45^oC
Initial Pressure: Vacuum [< 1.0x10^{-4} Torr]

The C-type thermocouple and convectron pressure transducer have been installed. The thermocouple is aligned so that it contacted the crushed ilmenite; at times it contacted the crucible wall.

The system was reduced to vacuum by an oil pump before the Fresnel lens was aligned. The vacuum pump was in continuous operation during the test. Once the focus was placed onto the ilmenite the temperature rapidly increased to 620^oC. At the same time the system pressure rose continually to 1.1x10^{-1} Torr. Both atmospheric conditions and misalignment of the focus decreased the chamber temperature and pressure to 532^oC and 2.4x10^{-2} Torr respectively. Later, the temperature increased from 450 to 610 ^oC, while the pressure increased from 3x10^{-3} to 2.9x10^{-2} Torr. The initial pressure response could be due to outgassing of trapped gasses and condensed water vapor. At one point, a rock split and part of it hit the window. Eventually the window cracked starting near the edge of the window. Upon removal, the crucible was cracked but held in place by the outer container.

The second test:
Initial Flux: 930 – 960 W/m^2
Peak Flux: 990 W/m^2
Initial Temperature: 96^oC
Maximum Temperature: >800^oC
Initial Pressure: Vacuum [< 1.0x10^{-4} Torr]

The C-type thermocouple was positioned carefully not to touch the window or to have both leads touching the walls of the chamber. The crucible was placed into the chamber without the larger crucible since the cracked crucible was presumed to occur due to different thermal expansion coefficients.

The chamber was pre-heated to 96^oC. As the pre-heating occurred, vapor condensed on the window, but slowly baked off as the temperature rose. Around 85^oC the window showed no sign of the vapor. The chamber was brought down to vacuum and it remained there for the duration of the test. No pressure increases were seen during this test. The ilmenite heated up and eventually "boiled." While the rocks were increasing in temperature, the crucible cracked and split into a number of pieces.

After the rocks cooled and the chamber was disassembled the rocks were analyzed. The rocks on the top (the ones that were boiling) were fused together and definitely showed signs of melting.

Mass properties:
Before test:

Crucible weight: 70.7187g
Crucible and ilmenite weight: 99.1128g
Ilmenite weight: 28.3936g

After test:

Rocks and crucible weight: 99.0668g
Rocks and dish: 62.5534g
Dish weight: 34.2039g

Calculations:

Rock weight after test: 28.3495g (in dish)
Rock weight after test: 28.3481g (in crucible)
Change in rock mass: 0.0441g ±0.0014
Percent mass change: 0.1553%

Laser Ilmenite test – Magnetic condenser

Work done by Brian Pomeroy

According to the Ward's Natural Science Establishment, Inc. ilmenite is easily distinguishable from "magnetite by its lack of strong magnetism," however, it also says that ilmenite is "magnetic after heating." Knowing that some of the products that are formed when heating the ilmenite to extreme temperatures are iron or iron rich compounds the idea of using a magnetic field to attract the material to an area for condensing. Other research shows that iron loses its magnetic strength as it is heated to temperatures above 600°C.

Two tests were conducted in order to determine if this would be a logical method for condensing. The first test consisted of a small piece of aluminum foil wrapped around the magnet. The particulate should condense onto the foil for massing. The magnet was placed in the chamber on the part of the cross that was towards the vacuum. The ilmenite rock had a mass loss of 0.0036g. The foil has a mass gain of 0.0001g, but the masses were within the range of the measurements. This means that the mass gain was too small to determine if it was actually condensed particulate or not.

The second test was conducted with two collectors, one with and one without a magnet. The aluminum foil without the magnet was placed on the way to the vacuum pump and the aluminum foil with the magnet was placed across the chamber where the thermocouple normally is located. With these tests, the ilmenite lost 0.0032g, but neither of the collectors showed a mass change.

Since neither of the tests showed an increase in mass it is believed that the laser is not vaporizing enough ilmenite to condense and show a mass change.

Outgassing Test

Brian Pomeroy

Three samples were tested for outgassing in different manors. The first sample was tested in an oven at atmospheric pressure and 120°C for two hours. The second sample was placed in a vacuum chamber for two hours, followed by heating at 700°C for two hours. The third and final sample was first heated to 700°C for two hours followed by two hours in the vacuum chamber. In each of the measurements the crucible was included in the outgassing calculations. Two crucibles were outgassed without any sample at 120°C to determine the total mass loss of the crucibles. The heated samples were allowed to cool before the mass was taken so the heat would not affect the mass.

Procedure:

The total mass loss (TML) and the percent total mass loss (%TML) for each of the tests was found and recorded. Each time the mass was determined five mass readings were averaged to determine the most accurate mass to the 0.0001g. To determine the TML, the average of the sample after the outgassing was subtracted from the original mass average. These masses included both the crucible and the ilmenite rock sample. The %TML was determined by dividing the TML by the original mass and multiplying by 100 for a percentage.

Crucible Outgassing Test

Brian Pomeroy

Two crucibles were outgassed for 1 hour and 20 minutes at 120°C. The TML was 0.0015% for each of the crucible samples. This is an extremely small amount, therefore not producing a substantial amount of mass loss to sample mass.

Ilmenite Outgassing Test

Brian Pomeroy

The first outgassing test simulated chamber preheating by heating the sample to 120°C for two hours. The TML for the ilmenite was 0.109%.

The next test was a vacuum test for 2 hours followed by heating to 700°C for two hours. The TML exhibited by the ilmenite was 0.0646% after the vacuum test. Next, the sample was subjected to heating and the final TML of the ilmenite was 0.504%.

The final test was to heat the sample first to 700°C then place it in a vacuum for 2 hours. The TML after the heating was 0.647%. After the vacuum test, the final TML was 0.601%. The sample possibly gained weight during the cooling process after heating. This gained mass was most likely not outgassed during the vacuum process.

Enstatite Outgassing Test

Brian Pomeroy

The first test simulating a pre-heating of the chamber heated the sample to 120°C for 2 hours. The TML for this sample was 0.162%.

The second test first pulled a vacuum on the sample for 2 hours. After the vacuum the sample's TML was 0.0356%. After the vacuum test, the sample was baked for 2 hours at 700°C. After the baking and cooling the sample exhibited a mass loss of 0.634% from just the heating. The TML of the entire test is 0.669%.

The final test was to heat the sample first to 700°C. After the heating the sample had a TML of 0.697%. Then it was placed in a vacuum for 2 hours. The TML of the entire run was 0.683%. The sample possibly gained weight during the cooling process after heating. This gained mass was most likely not outgassed during the vacuum process.

18 April 2005
Test 3
First attempt at 1330 canceled due to focus below chamber.

Second attempt at 1610
Solar flux: 890 W/m^2
Initial temperature: 27^oC
Initial pressure: 6e-1 Torr
Final pressure: 5e-1 Torr

The chamber was not pre-heated during this test. The chamber was decreased to 6e-1 Torr on the convectron gage using the Scroll pump. The leak valve on the chamber was closed to not allow any gases to go to the RGA. The thermocouple was placed into the ilmenite, but careful not to touch the sides of the crucible.

When the solar flux was concentrated into the chamber the temperature rose quickly then suddenly started to drop around 400^oC, simultaneously as the chamber pressure rose to 8e-1 Torr. The decrease in temperature was due to condensation forming on the window and blocking some of the sunlight to the sample. The condensation also explains the increase in pressure. After the condensation evaporated off the window the pressure dropped to 5e-1 Torr for the remainder of the test. The temperature increased to 620^oC when the crucible cracked. The temperature continued to rise and a small portion of the sample showed boiling. The glass window finally cracked at a little over 700^oC.

Ilmenite test mass:
Mass of crucible: 58.3494g
Mass of Ilmenite (start): 29.3357g
Mass of Ilmenite (end): 29.2258g
Delta mass: 0.1099g

3 May 2005
Test 4

ENSTATITE TEST AND WINDOW TEST

A new window was created with a 2 inch diameter fused silica window, 3 o-rings, and 2 flanges. The window was sandwiched between the two flanges with the o-rings sealing the vacuum chamber. Enstatite was used as the test sample for this test.

The chamber was pre-heated so the starting temp was 74°C. At 48°C and 4.4e-2 Torr, the sample began to outgas and condense on the window temporarily. The pressure also rose slightly before dropping again. The additional flange thickness made it difficult to heat the sample due to getting the focus into the chamber and onto the rocks. The window was slightly smaller than the previous ones used of 3 inches. As the chamber was heating up after being solar heated the o-ring began to smoke and melt before bursting into flames. The o-ring heated beyond its temperature rating. The test was ended at this point. No observable boiling was seen during the test and high temperatures were not reached, any mass loss is presumably from outgassing that occurred due to the low pressure and temperature.

Test Conditions:

- Starting time: 16:30
- Starting temperature: 74°C
- Flux: 956 W/m^2
- Pressure: 4.1 Torr
- Ending temperature: 548°C

Mass

- Average crucible mass: 72.2859 g
- Average crucible + enstatite mass: 82.1366 g
- Initial enstatite mass: 9.8508 g
- Final enstatite mass: 9.8458 g

- Mass change: 0.0508%

9 June 2005
Enstatite Fresnel Test
Test 5

Enstatite Test Early June

Observations
Enstatite $MgSiO_3$
Initial Flux: 924 - 950 W/m^2
Initial temperature: 50^{o}C
Initial Pressure: Vacuum [~ 1.4x10^{-1} Torr]
Instruments used: C-type thermocouple, Convectron pressure transducer

Preparation of the enstatite included grinding the rock into smaller pieces, however they were not as finely ground as previous ilmenite experiments. The sample was weighed three times previous to testing while in the crucible. The measurements only differed by 0.0003 grams each time the scale tared. The zirconia molded crucible and stand werer used to raise the sample near the window. The distance between the sample and window increased slightly from the ilmenite tests. This was due to the new zirconia molded stand instead of the pressed zirconia powder.

The chamber was reduced to 1.4 x 10^{-1} Torr with the scroll pump. Initially the scroll pump increased the pressure of the storage bottle. The pressure gradient slowed and nearly stopped the scroll pump. For operational considerations, the scroll pump must be turned on first, thus evacuating the main chamber. Once a good vacuum is established the storage bottle will be hooked to the roughing pump to ensure vacuum before the sample is subjected to the sun.

Test #	Mass (g)
Crucible Weight	
1	57.7936
2	57.7939
3	57.7938
4	57.7940
5	57.7942
Average	57.7939
Initial Enstatite + Crucible Weight	
1	68.8408
2	68.8413
3	68.8407
4	68.8413
5	68.8411
Average	68.8410
Starting Enstatite mass	
Average	11.0471

Ending Enstatite + Crucible Weight	
1	68.7524
2	68.7525
3	68.7528
4	68.7533
5	68.7530
Average	68.7528
Ending Enstatite mass	
Average	10.9589
Vaporization	
TML	0.0882
%TML	0.798759

16 June 2005
Aluminum Oxide Fresnel Test
Test 6

Incomplete Aluminum Oxide Test

Observations
Al_2O_3
Initial Flux: 950 W/m^2
Initial temperature: ~ 40^{o}C
Initial Pressure: Vacuum [~ 1.4x10^{-1} Torr]
Instruments used: C-type thermocouple, Convectron pressure transducer

Recent successful tests raised interest in the possibility of melting or vaporizing aluminum oxide. A large sample, approximately 19 grams, was placed into the large zirconia crucible. Previously, the white zirconia crucibles were used. Another stand was molded to allow for the larger crucibles. When the sample was placed into the vacuum chamber at least a gram was spilt. A decision was made to bake as much of the aluminum oxide as possible, regardless of vacuum or mass loss errors. The thermocouple had also dislodged from within the sample, moving it 2-3 mm above the surface of the powder.

The weather was partly cloudy, but yielded about 20 minutes of good solar exposure. Few notes and observations were made during this experiment; however, many lessons were learned. The technique in finding and applying the focus was drastically improved. Using the water spray to line up focus at the proper height with the chamber out of position is crucial. The fresnel lens must be aligned both by aligning the cart with the sun and also by tightening the focus onto the wood block, then fastening the wing-nuts on the lens into position. This fixes the setup so the chamber can easily be moved into and out of solar flux. Also, the person manning the chamber can used the reflection in the lens to determine if the focus is indeed on the sample. The use of the handheld mirror aids to provide a close and safe view of the sample when heated.

The 20 minutes of solar exposure rendered the aluminum oxide into a hot molten state. The glass window cracked after the first five minutes of exposure, but since the pressure did not rise past 3 Torr, the experiment continued. The thermocouple was in the direct center of the focus for the test. The thermocouple registered temperatures increasing to above 1600 degrees, with a purported 1800 as a maximum. Near that temperature the thermocouple melted and displayed "open" for the remainder of the test. About 1.5 cm of thermocouple was lost into the aluminum oxide. The experiment only ended when clouds restricted solar flux. At this time the molten picture was taken below. The sample was left to cool indoors. Once cool it was removed from the chamber. The sample had sintered together to form a large solid chunk of aluminum oxide. Once small fragment that was at the focus for the majority of the time had crystallized, but that region is very small in comparison to the sample. About 1/3 of the sample was melted together.

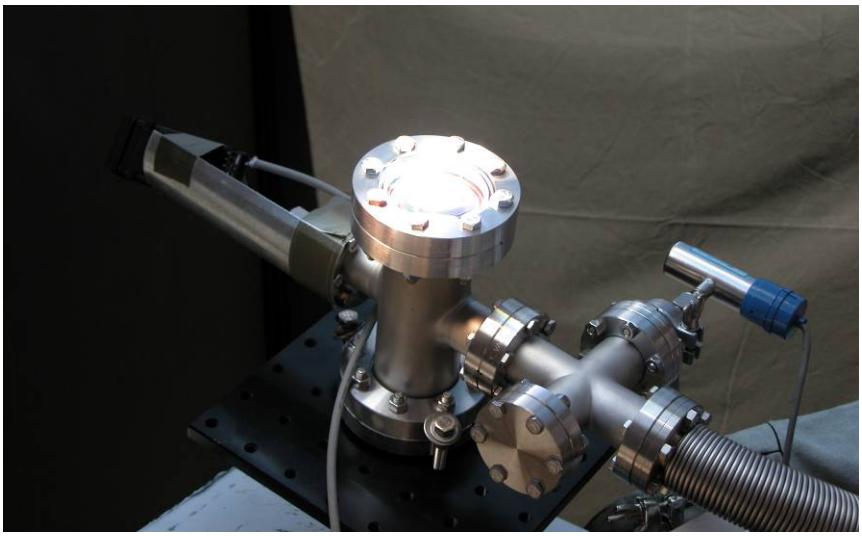

Chamber with focused radiation

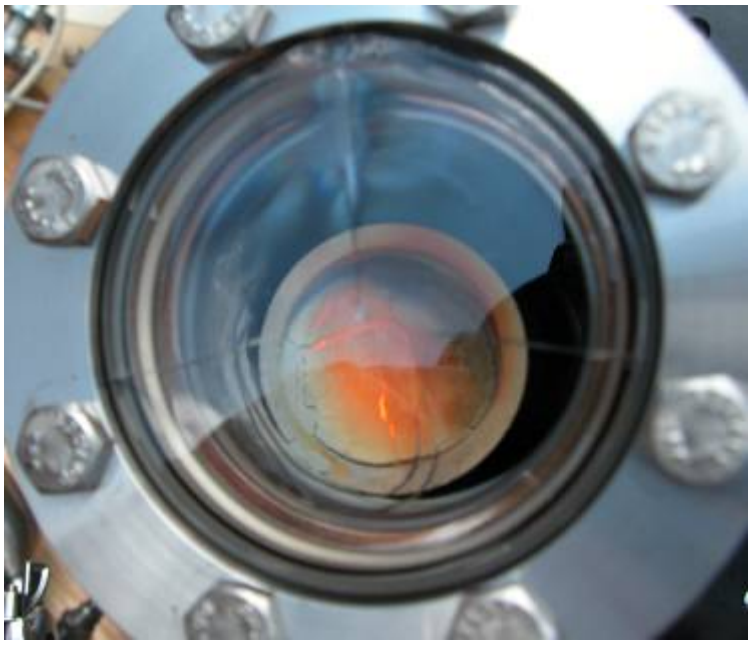

Molten Aluminum Oxide

17 June 2005
Ilmenite Fresnel Test
Test 7

Ilmenite Test

Observations

Initial Flux: 975 W/m^2
Initial temperature: ~ 40^{o}C
Initial Pressure: Vacuum [~ 2.3x10^{-1} Torr]
Instruments used: C-type thermocouple, Convectron pressure transducer

The weather was ideal to do a bake out test. Clear skies with low humidity provided nearly 1000 W/m^2 of solar flux. Since the motive was to provide the maximum solar exposure to ilmenite, a used window and thermocouple were employed. It was assumed that the window would break, so once again if the pressure did not increase above 5 Torr the experiment would not be stopped. The large zirconium crucible is far superior to that of the white zirconium. It withstood two tests totaling one hour and a half at temperatures near 1800 ^{o}C. The thermocouple was initially buried about 2-3 mm beneath the surface of the ilmenite. There was a period of lag between the sample heating and a register of temperature increase by the thermocouple. The thermocouple failed in this test at the 26th minute of exposure. The tip separated from the leads in the area near the sample/focus.

The following time log recorded observations: Start time 1:07 pm

Time	Flux (W/m^2)	Temperature(^{o}C)	Pressure(Torr)	Observations
0min00sec	970	35	3.9 x 10^{-1}	
2min30sec	975	580	6.8 x 10^{-1}	Boiling Began
7min30sec	975	930	4.1	Still boiling
10min00sec	950	1293	3.2	Isolated boiling
12min30sec	968	1190	3.2	
16min00sec	970	1185	3.5	
26min00sec	968	1867	3.4	Thermocouple lost
43min00sec	785	-open-	7.8 x 10^{-1}	Repositioning
59min00sec	987	-open-	1.2	

Ending just after 1 hour and seven minutes of exposure, the top surface of the sample was melted and had sintered together. A picture was taken soon after solar flux was removed; the ilmenite was in a molten state. Technique showed improvement in achieving high temperatures for extended periods of time. Future improvements include using a smaller sample mass to reduce the tendency of a heat sink.

This experiment was stopped because of the window. The picture below shows the window loosing viscosity as its temperature increased. The stress from the vacuum it contained was at a maximum at the center of the window. The window began to implode under the negative pressure. The test was called off for safety reasons.

Mass Properties
Average initial mass of ilmenite and crucible: 145.062 g
Average crucible mass: 106.1643 g
Average final mass of ilmenite and crucible: 144.880 g
Initial mass of ilmenite: 38.898 g
Final mass of ilmenite: 38.716 g
Mass loss: 0.182 g
Percent mass loss: 0.468%

A spectrum analysis was conducted with a SEM after the tests. The SEM showed that the relative amount of oxygen at the surface of the sample decreased between an unheated and heated sample of ilmenite. At the same time the relative amount of titanium at the surface increased. We would expect that there would be a decrease in oxygen and an increase in the metals after the sample was vaporized.

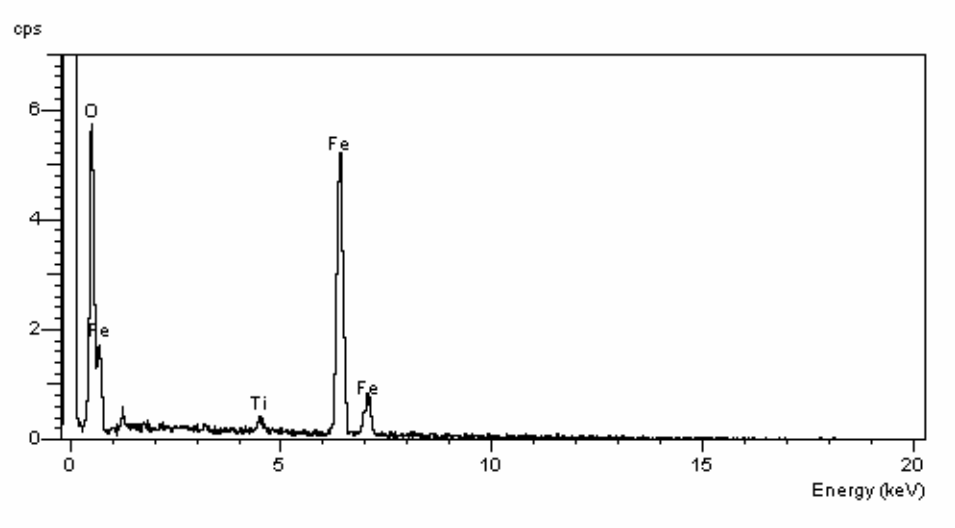

Pre-test ilmenite spectrum

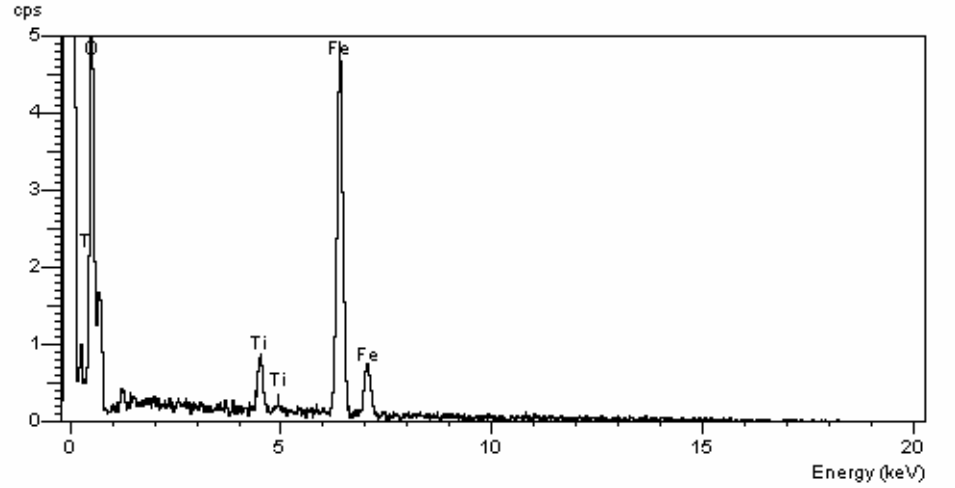

Post-test vaporized ilmenite spectrum

12 July 2005
Enstatie Fresnel Test
Test 8
$Mg_2Si_2O_6$

Enstatite Test

Observations

Initial Flux: 960 W/m^2
Initial temperature: ~ 40 ^oC
Initial Pressure: Vacuum [~ 7 Torr]
Instruments used: C-type thermocouple, Convectron pressure transducer, omega hand held pyrometer

This test was halted soon after the efficiency of the system was reduced from condensate on the inner surface of the vacuum window. It severely restricted the solar flux, thus reducing temperature and melt. A recommendation is put forth to add a condensing sheet to protect the windows from cracking so soon. The condensate was grayish in color, covering the majority of the lens. The longer the exposure time, the more cracks were formed. Establishment of a good vacuum was difficult. The chamber was pumped down to only about 7 Torr. This seemed to indicate a leak present in the system. The RGA was removed and precision leak valve shut tightly. The leak valve, even though it was shut, is likely to be the cause of leak. Normally, the system is able to attain a $1x10^{-1}$ Torr vacuum.

The following time log recorded observations: Start time 10:30 am

Time	Flux (W/m^2)	Temperature(^oC)	Pressure(Torr)	Observations
0min00sec	955	35	7	
2min45sec	945	580	10	Window Crack
5min30sec	955	1300	10	Boiling Began
30min00sec	950	900-1100	10	Test Terminated

Even though the test was cut short due to a lack of efficient energy transfer, it was highly successful. Enstatite yields a much higher mass loss than aluminum oxide or ilmenite. A ten percent mass loss gives hope to achieve larger partial pressures of oxygen production per gram of lunar soil.

In a comparison between all three minerals yields the conclusion that isolated temperatures above 1100 oC are needed to melt/boil the samples.
Mass Properties
Average initial mass of enstatite and crucible: 118.19 g
Average crucible mass: 107.576 g
Average final mass of enstatite and crucible: 117.058 g
Initial mass of enstatite: 10.614 g
Final mass of enstatite: 9.482 g
Mass loss: 1.132 g
Percent mass loss: 10.66%

27 July 2005 2:45 pm
Ilmenite Fresnel Test
Test 9
$FeTiO_3$

Ilmenite Test

Observations
Initial Flux: 780-807 W/m^2
RGA Start Time: 3:12
Initial temperature: ~ 40 ^oC
Initial Chamber Pressure: Vacuum [~ $6.6x10^{-2}$ Torr]
Instruments used: C-type thermocouple, Convectron pressure transducer, omega hand held pyrometer, MKS residual gas analyzer, ion gauge

This was the first pyrolysis test to include an active residual gas analyzer. The weather was very hot and humid, only providing 750 watts per square meter on average. The air was saturated with water vapor, causing a thick haze to be present. The test was conducted about four hours prior to a large thunderstorm. The humidity definitely reduces the spectral irradiance available for heating.

A reflective film was placed above the metal surface and screw heads exposed to the cone of concentrated sunlight. This film did not protect the window and steel from excessive heating. An investigation has begun to understand the coefficients of thermal expansion of the stainless steel and glass according to the stress concentrations at the screw holes and o-ring joints.

The maximum temperature reached in this test, measured by the thermocouple, was 1300^oC. A tight focus was seldom achieved on the surface of the ilmenite. The test arm was continuously raised to align with the focus. As with the last test, it remained difficult to work with the handheld pyrometer.

The RGA worked very well. There was a disagreement between the ion gauge and RGA total pressure measurement. In one instance the RGA measured a local pressure of $9.4x10^{-6}$ Torr while the ion gauge displayed $4.1x10^{-5}$ Torr. This disagreement has not been resolved; however, the RGA was just serviced a week ago and ion gauge has not been re-certified. The leak valve was altered twice during testing to allow the maximum leakage while preventing an over pressurization.

Mass loss was minimal due to the short exposure times at high temperatures. This test did provide a good exposure to the RGA. Other items of interest are the fast cracking of the windows the past few tests. Previously, tests lasted longer before cracking while at higher temperatures. This recent phenomenon is troubling. Suggestions for fixing this problem could be actively and passively cooling the steel to reduce thermal stresses on the window. The coefficient of steel is twice that of glass. We believe thermal expansion is causing large enough stress concentrations at the joints between the steel and glass to crack the glass.

The following time log recorded observations: RGA start time 3:12 pm

Time [RGA mark]	Flux (W/m^2)	Temp (^oC)	Chamber/RGA Pressure(Torr)		Observations
3:12	798	~40			RGA Start
3:18 [3.5]	750			$4.1x10^{-5}$Ion	RGA measuring $9.4x10^{-6}$ Torr Leak Valve Opened
3:20 [9]	750		$6.6x10^{-2}$		Test Start
3:22	~750		$1.2x10^{-1}$		
3:23	~750	1020	$1.5x10^{-1}$		
3:24	~750	1050	Temp Increase as focus acheived		
3:25	~750		9.2	Spike	**Window Breaks/RGA Stop**
3:27	732	1040			
3:28		1078			
3:31	745	1220			
3:33	738	1300	6.4	$5.2x10^{-4}$ Ion	
3:35	~750	1330	505	$6.4x10^{-4}$ Ion	RGA Restart
3:37 [2]	750	1050			Adjusting Leak Valve
3:38	~750	1100			
3:40 [5]	600				Short Shade overhead
3:42	732	850	2.6	$6.4x10^{-5}$ RGA	
3:44 [9.5]	~750				Chamber Moved
3:45	~750	H_2O concentration rose while O_2 reduced by half order of magnitude			
3:46 [12]	~750				Lens Safe
3:48	~750	486			Lens Safe and cloud
3:54 [19.5]	720				Lens and sun active
[25]	680				Adjusted focus until test stop

Mass Properties and Variations with Temperature
Initial Measurement at Ambient Conditions:

Average initial mass of ilmenite and crucible: **125.062g**
Average crucible mass: **107.576g**

Post Test Measurement at ~350^{o}C; 12 minutes after sun removed:

Average final mass of ilmenite and crucible: **124.918g**

Post Test Measurement at ~0^{o}C; 1 hour after test:

Average final mass of ilmenite and crucible: **124.979g**

Post Test Measurement at ~room temperature; 21hours after sun removed:

Average final mass of ilmenite and crucible: **124.934g**

Average initial mass of ilmenite (ambient conditions): 17.486 g
Average final mass of ilmenite (ambient conditions): 17.358g

Mass loss: 0.128 g
Percent mass loss: 0.73%
RGA Output and Comments

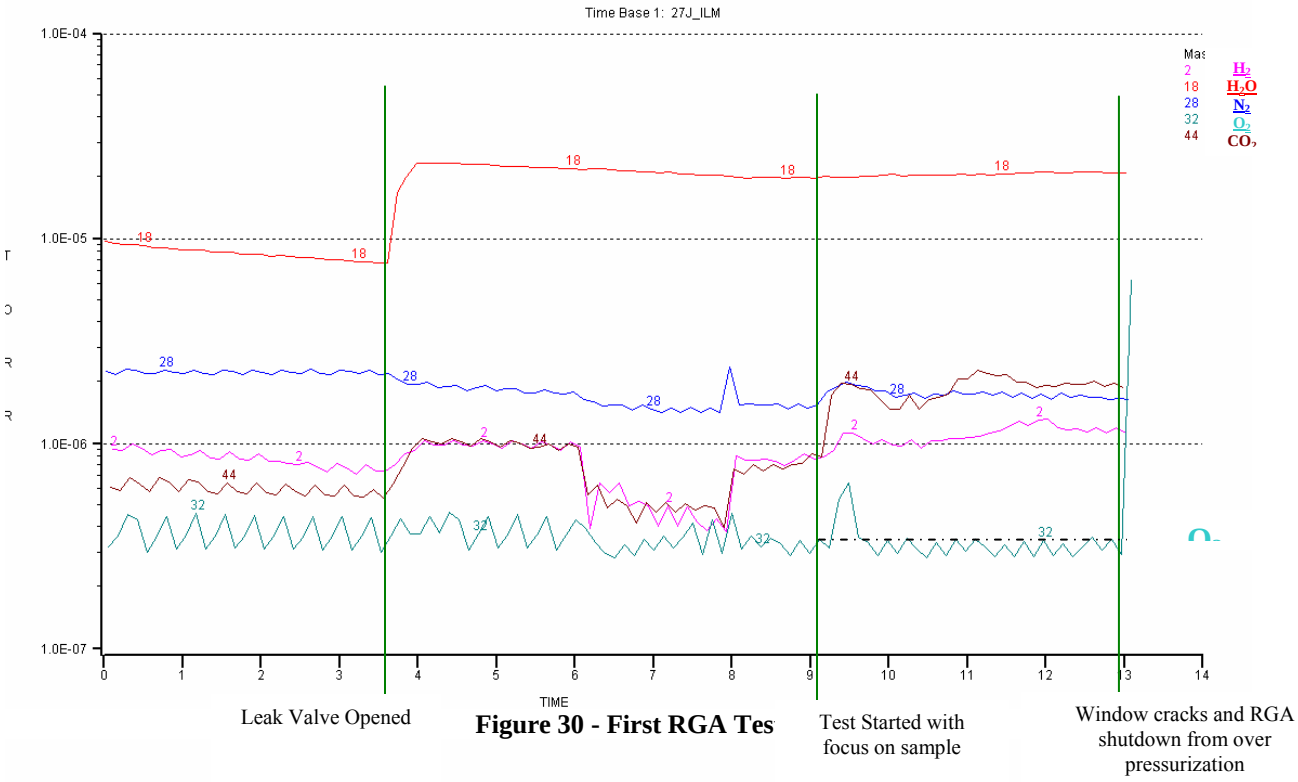

Figure 30 - First RGA Tes

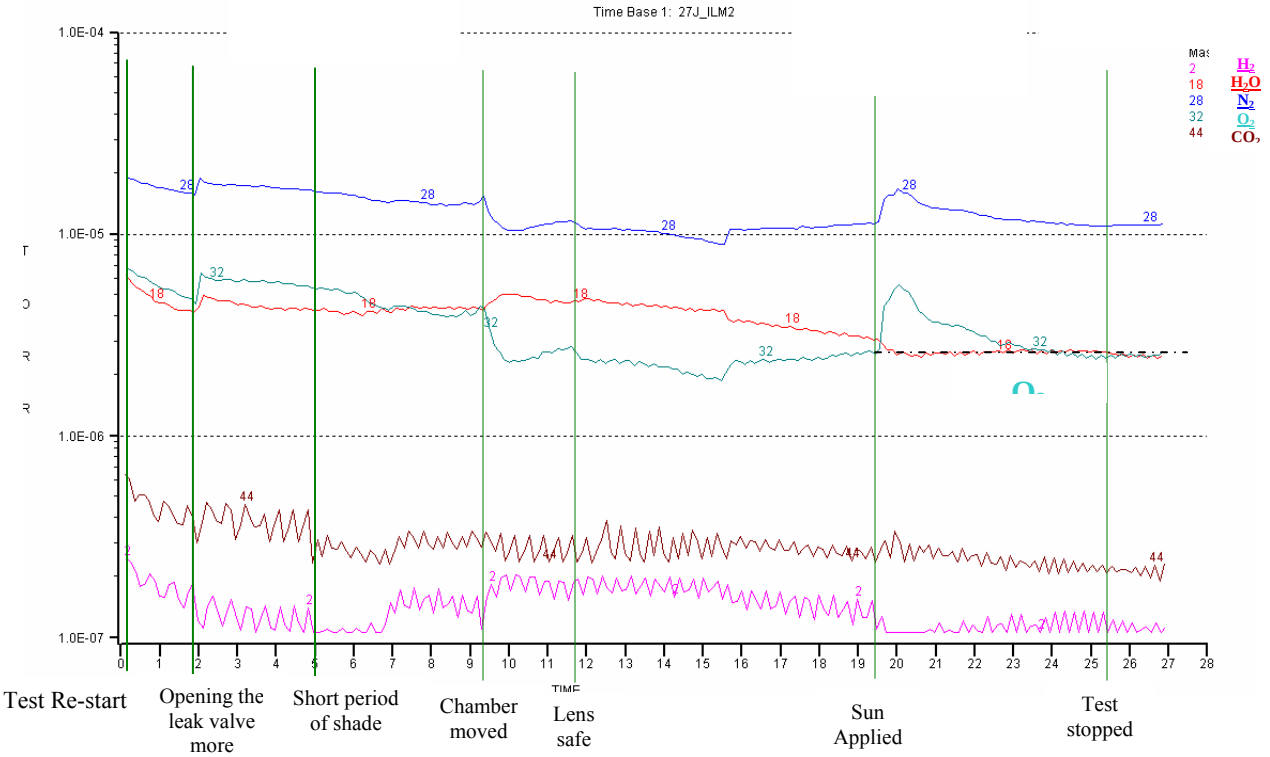

Figure 31 - Test Restarted with cracked window (partial pressure vs. time)

August 2005 10:30 am
Ilmenite Fresnel Test
Test 10
$FeTiO_3$

Ilmenite Test

Observations
Initial Flux: 880 W/m^2
RGA Start Time: 10:37
Initial temperature: ~ 22 ^oC
Initial Chamber Pressure: Vacuum [~ 1.4 Torr]
Max Temperature: 1436°C
Instruments used: C-type thermocouple, Convectron pressure transducer, omega hand held pyrometer, MKS residual gas analyzer, ion gauge, fan, LN_2 dewar

After the last successful failed test, it was determined that the window was heating to high temperatures while the steel was remaining warm. This thermal gradient is what most likely is causing the cracking to occur. So during this test first a fan was used to keep cool air passing over the chamber and window, and the second was blowing LN_2 vapor over the window. Despite trying to lengthen the time before cracking, the window lasted 12 minutes before cracking. It is believed that the window continues to crack due to the thermal temperature in the window, not necessarily the steel.

To help reduce the thermal shock to the system, a piece of cardboard was placed over the lens and slowly removed. This removal process took 4 minutes. The temperature in the chamber after removal of the cardboard was 500°C. The window temperature was around 100°C to 200°C when the window broke in the part of the window where material was not condensing. In the area where material was condensing the temperature reached 250°C to 300°C when the window broke. It is believed that the window keeps breaking due to the thermal gradients in the window as it heats up. These gradients could be caused by condensed matter on the window.

The flux and temperature on this test was not the greatest due to the condensed matter on the window blocking the entering flux and the fact that a tight focus was not held on the sample as well as in past tests. This created a lower temperature which is reflected in the % of the material that was lost during the test.

As the test progressed, material began to condense on the window where the LN_2 vapor was blowing most. This area was in the center of the window as with past windows. This area became pronounced one minute before the window cracked (15 minutes). A SEM of this portion of the window will be conducted to determine the condensed species.

The first boiling was observed during the 8 minute mark. The melting of the ilmenite fused a portion of the rock together. The chamber pressure during this test was always around 1.4 Torr. The reason for this is most likely the pump. The RGA pressure was kept around $8x10^{-6}$ Torr.

This allowed for a slight increase of pressure when the window broke to continue taking measurements.

Initial mass:
Average Crucible mass: 106.5361g
Average crucible and ilmenite mass: 122.594g
Average ilmenite mass: 16.058g

Final mass:
Sample was spilt before massing
Average final mass: 122.535g
Average final ilmenite mass: 15.999g

Mass Loss:
Mass loss: 0.059g
%mass loss: 0.367%

Recorded observations: The RGA start time was 10:37 am.

Time of day (hh:mm:ss)	T+ (min)	Flux	Chamber Temp (°C)	Window temp - clear (°C)	Window Temp - Condensed (°C)	Steel window temp (°C)	Chamber / RGA pressure (Torr)		Comments
10:37	0	880							
10:39	2						1.4	2.30E-06	
10:40	3		22						
10:42	5		125	27		22	1.4	2.20E-06	
10:43	6		500				1.4	2.20E-06	
10:44:05	7								Tailoring focus
10:44:30	7		630						boiling
10:45:30	8		862		94	36			
10:46:15	9		1220						
10:47:00	10								Increased leak to RGA
10:47:40	10		1300						
10:48:00	11								Increase leak to RGA
10:49:00	12		1200	150		80	1.7	8.00E-06	
10:50:30	13		1200	100	250	45	1.8	8.60E-06	
10:51:29	14						7.1	2.30E-05	***Window broke***
10:53:10	16		1000	200	300	67	6.7	2.20E-05	
10:55:00	18	876	1150						
10:55:43	18		1200						
10:56:20	19		800	200	290	70	5.4	2.00E-05	Boiling ceased
10:58:50	21			250	300	110	4	1.60E-05	
11:02:28	25						5.7	2.00E-05	Re-align begin
11:06:55	29	880	880						Re-align end
11:08:10	31		900						
11:08:50	31	885	1000	220	250	100	4.4	1.60E-05	
11:12:00	35		973						
11:16:00	39	***END***							

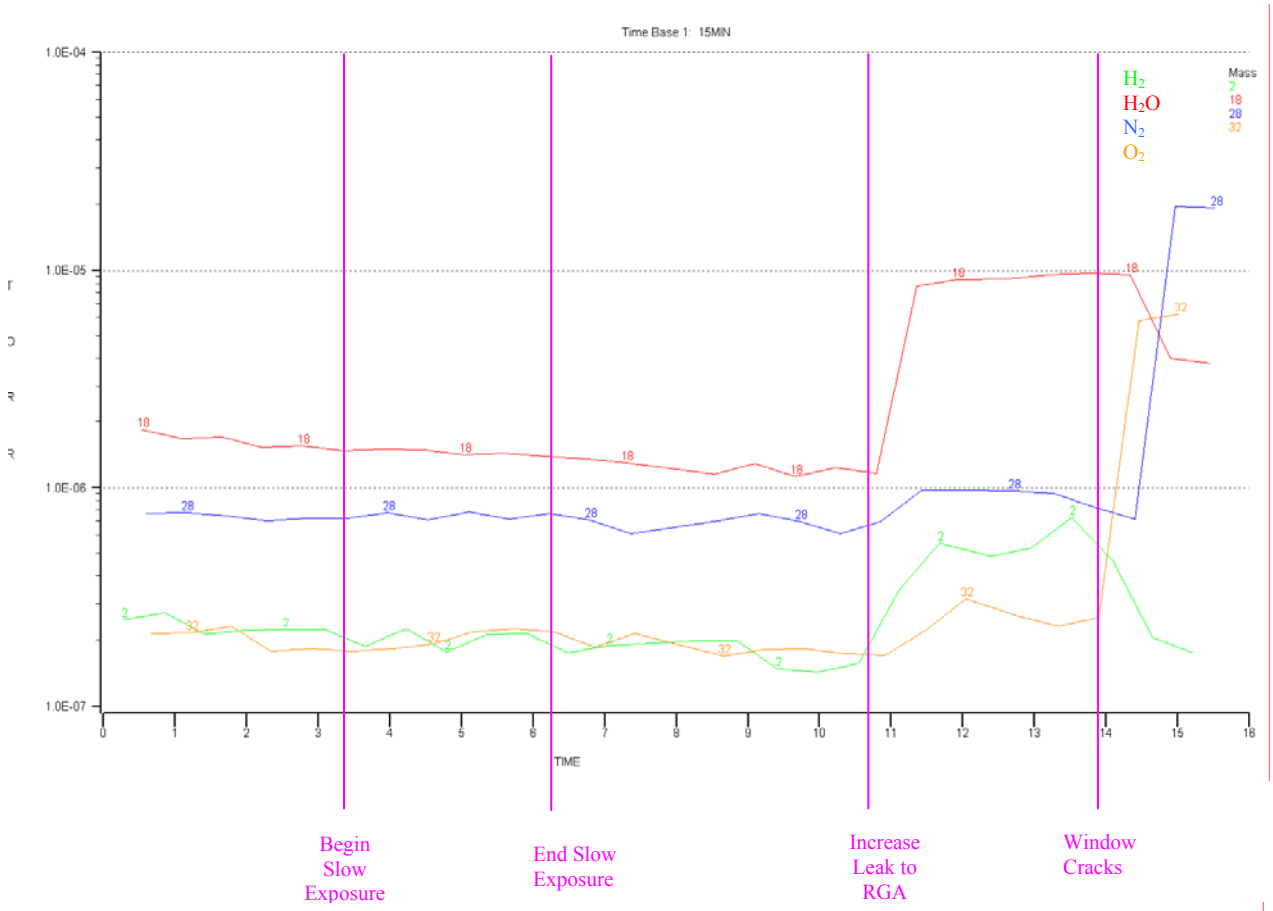
Time Base 1: 15MIN
1.0E-04
1.0E-05
1.0E-06
1.0E-07
TIME
H2
H2O
N2
O2
Mass
2
18
28
32
Begin Slow Exposure
End Slow Exposure
Increase Leak to RGA
Window Cracks

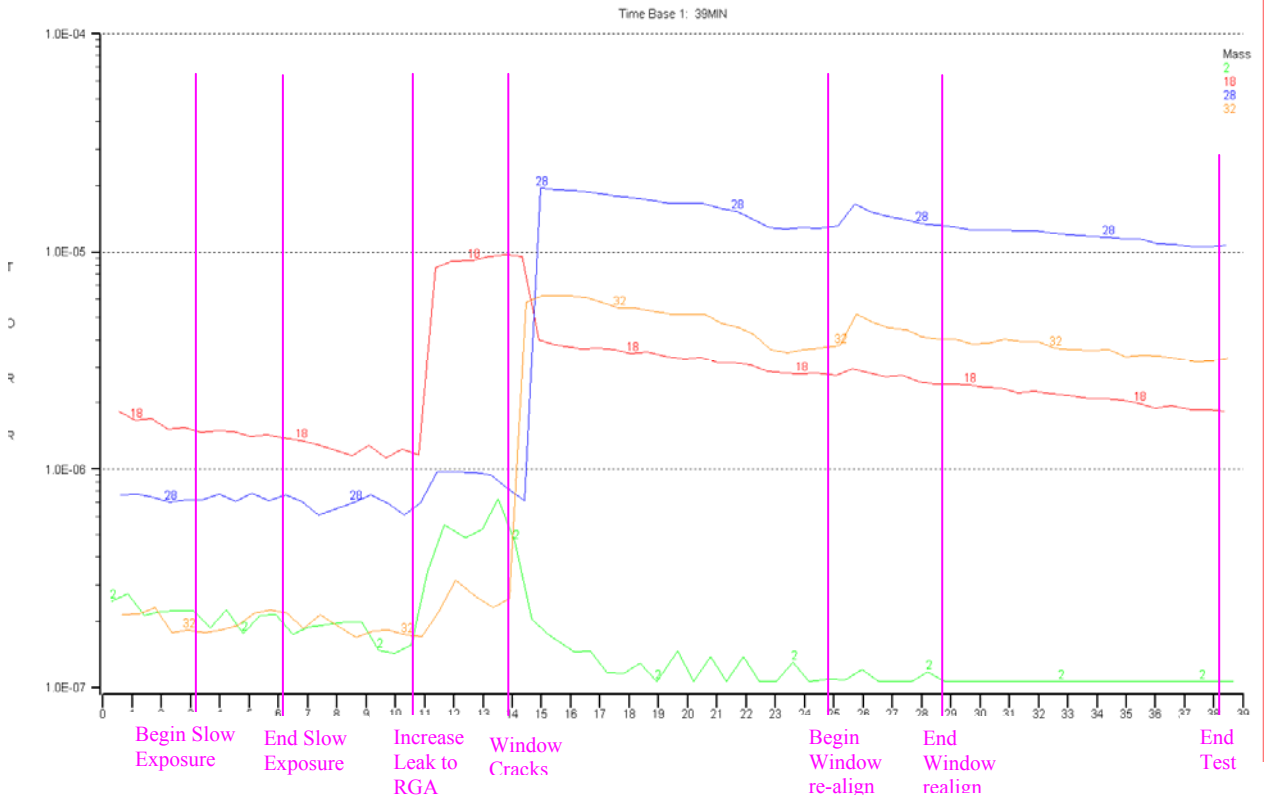
Time Base 1: 39MIN
1.0E-04
1.0E-05
1.0E-06
1.0E-07
Mass
2
18
28
32
Begin Slow Exposure
End Slow Exposure
Increase Leak to RGA
Window Cracks
Begin Window re-align
End Window realign
End Test

25 August 2005 11:54 am
MLS-1 Fresnel Test
Test 11
Mare Regolith Simulant

MLS-1A Test

Observations
Initial Flux: 1008 W/m^2
RGA Start Time: 12:02
Initial temperature: ~ 55 ^oC
Initial Chamber Pressure: Vacuum [~ $9.6x10^{-2}$ Torr]
Max Temperature: 1474°C
Instruments used: C-type thermocouple, Convectron pressure transducer, omega hand held pyrometer, MKS residual gas analyzer, ion gauge

This test was the first of the lunar regolith simulant referred to as MLS-1. MLS-1 is a comparative to the Apollo 11 sample number 10087 from the sea of tranquility in terms of chemistry. The simulant is completely crushed to a powdery substance. Its geological characteristics vary from lunar soil having less glass content and no atomic iron content. This was also the first Fresnel test at the propulsion test site and the first test with the operational water cooler/chamber wall condenser.

Once concentrated sunlight was exposed to the simulant, the chamber pressure increased to 1.4 $x10^{-1}$ Torr. Melting, followed immediately by boiling was observed at the second minute while the thermocouple measured 1320^oC. The thermocouple measured temperatures between 850-980^oC in the third and fourth minutes. During this time the secondary window, placed directly over the crucible, became completely covered in condensation. In the fifth minute of operation the vacuum-sealed window cracked and chamber pressure rose to $6.4x10^{-1}$ and climbed slowly ($0.5x10^{-1}$ Torr every 30 seconds). The simulant continued to boil despite the condensation on the protective window. Measurements of the chamber wall and window measured 190^oC and 200^oC respectively with the IR thermometer. The increase in chamber pressure caused the RGA to overpressure, which automatically shuts it down.

The remainder of the test was a bakeout test to determine mass loss of the system. Solar flux remained constat at 990-1020 W/m^2. Chamber pressure rose to an equilibrium of 3.1 Torr with a chamber temperature of 1140^oC at about eight minutes into the test. The secondary window became clearer near the ten minute mark while the main window continued to crack. Boiling continued at 1200^oC through fifteen minutes. From fifteen minutes to fifty two minutes the chamber temperature altered between 900-1200 on average with periods of maxima at 1440^oC. The test was halted at fifty two minutes when boiling settled.

Initial mass:
Average Crucible mass: 76.0526 g
Average crucible and simulant mass: 85.0394 g
Average ilmenite mass: 8.987 g

Final mass:
Crucible was broken in attempt to free from sintered thermocouple. Error with small missing crucible pieces and thermocouple addition.
Average final mass: 84.1315 g
Average final simulant mass: 8.079 g

Mass Loss:
Mass loss: 0.908g
Percent mass loss: 10.1 %

Secondary Window (Protection) with condensation : 18.9022 g